

This discussion paper is/has been under review for the journal Hydrology and Earth System Sciences (HESS). Please refer to the corresponding final paper in HESS if available.

Recent developments in predictive uncertainty assessment based on the model conditional processor approach

G. Coccia and E. Todini

Department of Earth and Geo-Environmental Sciences, University of Bologna, Bologna, Italy

Received: 17 November 2010 – Accepted: 24 November 2010 – Published: 6 December 2010

Correspondence to: G. Coccia (gabriele.coccia4@unibo.it)

Published by Copernicus Publications on behalf of the European Geosciences Union.

HESSD

7, 9219–9270, 2010

Recent developments in predictive uncertainty assessment

G. Coccia and E. Todini

Title Page

Abstract

Introduction

Conclusions

References

Tables

Figures



Back

Close

Full Screen / Esc

Printer-friendly Version

Interactive Discussion

Abstract

The work aims at discussing the role of predictive uncertainty in flood forecasting and flood emergency management, its relevance to improve the decision making process and the techniques to be used for its assessment.

5 Real time flood forecasting requires taking into account predictive uncertainty for a number of reasons. Deterministic hydrological/hydraulic forecasts give useful information about real future events, but their predictions, as usually done in practice, cannot be taken and used as real future occurrences but rather used as pseudo-measurements of future occurrences in order to reduce the uncertainty of decision makers. Predictive
10 uncertainty (PU) is in fact defined as the probability of occurrence of a future value of a predictand (such as water level, discharge or water volume) conditional upon prior observations and knowledge as well as on all the information we can obtain on that specific future value from model forecasts. When dealing with commensurable quantities, as in the case of floods, PU must be quantified in terms of a probability distribution function which will be used by the emergency managers in their decision process in
15 order to improve the quality and reliability of their decisions.

After introducing the concept of PU, the presently available processors are introduced and discussed in terms of their benefits and limitations. In this work the Model Conditional Processor has been extended to the possibility of using a joint truncated
20 normal distribution, in order of improving adaptation to low and high flows.

The paper concludes by showing the results of the application of the MCP on the Baron Fork River, OK, USA. The data set provided by the NOAA's National Weather Service, within the DMIP 2 Project, allowed two physically based models, the TOPKAPI model and TETIS model, to be calibrated and a data driven model to be implemented
25 using the Artificial Neural Network. The three model forecasts have been combined with the aim of reducing the PU and improving the probabilistic forecast taking advantage of the different capabilities of each model approach.

Recent developments in predictive uncertainty assessment

G. Coccia and E. Todini

Title Page

Abstract

Introduction

Conclusions

References

Tables

Figures



Back

Close

Full Screen / Esc

Printer-friendly Version

Interactive Discussion



1 Introduction

1.1 Decision making under uncertainty

In the last decades, the interest in assessing uncertainty in models forecasts has grown exponentially within the scientific communities of meteorologists and hydrologists. In particular, the introduction of the Hydrological Uncertainty Processor (Krzysztofowicz, 1999; Krzysztofowicz and Kelly, 2000), aimed at assessing predictive uncertainty in hydrological forecasts, has created the basis for the estimation of flood predictive uncertainty.

Flood emergency management requires adopting operational decisions in real time that may lead to dramatic consequences (economical losses, casualties, etc.). The hardest obstacle the managers have to deal with is the uncertainty on the future evolution of events. Decision theory (De Groot, 1970; Raiffa and Schlaifer, 1961) studied this problem and provided the most appropriate solutions for taking decisions under uncertainty. This approach consists in minimizing the expected value of a utility function $U(y)$ representing the losses, or more in general the manager perception of them, as a function of a predictand that will occur at a future time (such as a future discharge or water stage in a cross section). This quantity is unknown at the time of the decision (t_0) and the aim of forecasting is to assess its probability of occurrence, in terms of a predictive uncertainty probability density function.

In the case of flood forecasting, predictive uncertainty can be defined as the uncertainty that a decision maker has on the future evolution of a predictand that he uses to make a specific decision.

In order to fully understand and to appreciate what is actually meant by predictive uncertainty, it is necessary to realize that what will cause the flooding damages is the actual future realization of the discharge and/or the water level that will occur, not the prediction generated by a forecasting model; in other words the damages will occur when the actual water level y_t and certainly not if the prediction \hat{y}_t will overtop the dyke

Recent developments in predictive uncertainty assessment

G. Coccia and E. Todini

Title Page

Abstract

Introduction

Conclusions

References

Tables

Figures



Back

Close

Full Screen / Esc

Printer-friendly Version

Interactive Discussion



level y_D (Todini, 2009). Therefore a utility/damage function at any future time ($t > t_0$) must be expressed as a function of the actual level that will occur at time t

$$\begin{cases} U(y_t) = 0 & \forall y_t \leq y_D \\ U(y_t) = g(y_t - y_D) & \forall y_t > y_D \end{cases} \quad (1)$$

where $g(\cdot)$ represents a generic function relating the cost of damages and losses to the future, albeit unknown water stage y_t . In this case the manager, according to the decision theory (De Groot, 1970; Raiffa and Schlaifer, 1961), must take his decisions on the basis of the expected utility $E\{U(y_t)\}$. This value can be estimated only if the probability density function of the future event is known, and it can be written as

$$E\{U(y_t)\} = \int_0^{+\infty} U(y_t) f(y_t) dy_t \quad (2)$$

where $f(y_t)$ is the probability density expressing our incomplete knowledge (in other words our uncertainty) on the future value that will occur. This density, which can be estimated from historical data, is generally too broad because it lacks the conditionality on the current events. This is why it is essential to improve this historical probability distribution function by more realistically using one or more hydrological models able to summarize all the available information (like the rain forecast, the catchment geomorphology, the state of the river at the moment of the forecast, etc. . .) and to provide a more informative density $f(y_t | \hat{y}_{t|t_0})$, which expresses our uncertainty on the future predictand value after knowing the models' forecasts issued at time t_0 , namely $\hat{y}_{t|t_0} = [\hat{y}_{1|t_0}, \hat{y}_{2|t_0}, \dots, \hat{y}_{M|t_0}]$, where M is the number of forecasting models. Equation (2) can now be rewritten as

$$E\{U(y_t | \hat{y}_{t|t_0})\} = \int_0^{+\infty} U(y_t) f(y_t | \hat{y}_{t|t_0}) dy_t \quad (3)$$

**Recent developments
in predictive
uncertainty
assessment**

G. Coccia and E. Todini

Title Page	
Abstract	Introduction
Conclusions	References
Tables	Figures
⏪	⏩
◀	▶
Back	Close
Full Screen / Esc	
Printer-friendly Version	
Interactive Discussion	



The probability distribution function $f(y_t|\hat{y}_{t|t_0})$ represents the PU, hereafter denominated $f(y|\hat{y})$ for sake of simplicity.

Summarizing, for a decision maker to take rational decisions it is necessary first of all to define his propensity to risk (e.g. the decision-maker could be risk-prone when the level of damage is low or risk-averse when the level of damage is high), which afterwards can be included in the chosen utility function, and then try to minimize the expected value of this risk on the basis of a predictive density function conditional on all the information he/she can gather and in particular on the available model forecasts. In this paper the available uncertainty processors (UPs) will be discussed, focusing on the Model Conditional Processor (MCP) (Todini, 2008) and highlighting the problem of the error heteroscedasticity and how to tackle it.

1.2 The probabilistic threshold paradigm

Today, similarly to what was done for more than a century, in order to trigger their decisions, the majority of water authorities involved in flood emergency management prepare their plans on the basis of pre-determined water depths or thresholds ranging from the warning water level to the flooding level. Decisions, and consequent actions, are then taken as soon as a real time measure of the water stage overtops one of these thresholds. This approach, which is correct and sound in the absence of flood forecasting models is a way of anticipating events on the basis of water level measures (in the cross sections of interest or in upstream cross sections), but can only be effective on very large rivers where the time lag between the overtopping of the warning and the flooding levels is sufficiently large to allow for the implementation of the planned flood relief strategies and interventions (Todini and Coccia, 2010).

Given that all the water stage measures are affected by relatively small errors (1–2 cm), they can be, and have been, considered as deterministic; therefore in the sequel this approach will be referred to as the deterministic threshold paradigm.

Recent developments in predictive uncertainty assessment

G. Coccia and E. Todini

Title Page

Abstract

Introduction

Conclusions

References

Tables

Figures

⏪

⏩

◀

▶

Back

Close

Full Screen / Esc

Printer-friendly Version

Interactive Discussion



2 Existing approaches

2.1 Hydrological uncertainty processor

Krzysztofowicz (1999) introduced a Bayesian processor, the Hydrological Uncertainty Processor (HUP) which aims at estimating the predictive uncertainty given a set of historical observations and a hydrological model prediction. The HUP was developed around the idea of converting both observations and model predictions into a normal space by means of the NQT in order to derive the joint distribution and the predictive conditional distribution from a treatable multivariate distribution. In practice, as described in Krzysztofowicz (1999), after converting the observations and the model forecasts available for the historical period into the normal space, the HUP combines the prior predictive uncertainty (in this case derived using an autoregressive model) with a Likelihood function in order to obtain the posterior density of the predictand conditional to the model forecasts. From the normal space this conditional density is finally re-converted into the real space in order to provide the predictive probability density.

The introduction of HUP generated a positive impact into the hydrological community, because it was the first time that predicting uncertainty was correctly formulated and used in hydrological forecasting. Nonetheless, HUP has three major limitations. The first one relates to the fact that only one model at a time can be used in HUP, which is hardly extendable to multi model forecasts. Moreover the used prior autoregressive (AR) model frequently tends to be inadequate to represent the predictand, as for instance in the case of a flood routing problem where the AR model is adequate for representing the recession but not the rising limb of the flood wave. Finally, the HUP procedure implies the independence of the AR model errors from those deriving from the used prediction model, which is not guaranteed due to the fact that both models tend to be highly correlated to the observations, which inevitably induces a level of correlation among them.

Recent developments in predictive uncertainty assessment

G. Coccia and E. Todini

Title Page

Abstract

Introduction

Conclusions

References

Tables

Figures



Back

Close

Full Screen / Esc

Printer-friendly Version

Interactive Discussion



2.2 Bayesian model averaging

Introduced by Raftery (1993), Bayesian Model Averaging (BMA) has gained a certain popularity in the latest years. The scope of Bayesian Model Averaging is correctly formulated in that it aims at assessing the mean and variance of any future value of the predictand conditional upon several model forecasts. Differently from the HUP assumptions, in BMA all the models (including the AR prior model) are similarly considered as alternative models. Raftery et al. (2005) developed the approach on the assumption that the predictand as well as the model forecasts were approximately normally distributed, while Vrugt and Robinson (2007) relaxed this hypothesis and showed how to apply the BMA to Log-normal and Gamma distributed variables. In practice the Bayesian Inference problem, namely the need for estimating a posterior density for the parameters, is overcome in the BMA by estimating a number of weights via a constrained optimization problem. Once the weights have been estimated, BMA allows to estimate the mean and the variance of the predictand conditional upon several models at the same time.

The original BMA, as introduced by Raftery (1993), has shown several problems. First of all, as pointed out by Vrugt and Robinson (2007), the original assumption of approximately normally distributed errors, is not appropriate for representing highly skewed quantities such as water discharges or water levels in rivers. Therefore one must either relax this hypothesis, as done by Vrugt and Robinson (2007) who applied the BMA to Log-normal and Gamma distributed variables or to convert the original in the normal space once again using the NQT, as done in Todini (2008). Another problem, which emerges from the application of BMA is the use of the “expectation-maximization” (EM) algorithm (Dempster et al., 1977) proposed by Raftery et al. (2005), which was not found to properly converge to the maximum of the likelihood. To overcome this problem, one can either use sophisticated, complex optimization tools such as the SCEM-UA (Vrugt et al., 2003) or, as proposed by Todini (2008), a simple and original constrained Newton-Raphson approach, which converges in a very limited

Recent developments in predictive uncertainty assessment

G. Coccia and E. Todini

Title Page

Abstract

Introduction

Conclusions

References

Tables

Figures



Back

Close

Full Screen / Esc

Printer-friendly Version

Interactive Discussion



number of iterations.

2.3 Model conditional processor

The Model Conditional Processor (MCP) is a Bayesian methodology, proposed by Todini (2008), for estimating the predictive uncertainty. The derivation of the predictive distribution is essentially based on the estimation of a joint predictand-prediction distribution, computed by taking advantage of the model behaviour knowledge acquired through the available historical series. Since the multivariate distributions can be formulated and effectively analytically treated in a very limited number of cases, Krzysztofowicz (1999) suggested transforming the observations and model forecasts in a Gaussian or normal space via a non parametric transformation known as the Normal Quantile Transform (NQT) (Van der Waerden, 1952, 1953a,b). The NQT allows the observation y and the model forecast \hat{y} to be converted into a normal space using the quantiles associated to the order statistics, computed by means of the Weibull plotting position.

The original variables y and \hat{y} are so converted to their transformed values η and $\hat{\eta}$, respectively, which are distributed with a normal standard distribution, and the probability of each element is the same as its original corresponding value. So the relation between the original variables and their transformed values is

$$P(y < y_i) = \frac{i}{n+1} = P(\eta < \eta_i), \quad \text{for } i = 1, \dots, n,$$

where n is the number of the historical available data and i the plotting position order.

In the normal space the joint distribution of η and $\hat{\eta}$ can be assumed as a normal bivariate, $f(\eta, \hat{\eta})$, with mean and variance

$$\boldsymbol{\mu}_{\eta, \hat{\eta}} = \begin{bmatrix} 0 \\ 0 \end{bmatrix} \quad (4)$$

$$\boldsymbol{\Sigma}_{\eta, \hat{\eta}} = \begin{bmatrix} 1 & \sigma_{\eta \hat{\eta}} \\ \sigma_{\eta \hat{\eta}} & 1 \end{bmatrix} \quad (5)$$

Recent developments in predictive uncertainty assessment

G. Coccia and E. Todini

Title Page

Abstract

Introduction

Conclusions

References

Tables

Figures

⏪

⏩

◀

▶

Back

Close

Full Screen / Esc

Printer-friendly Version

Interactive Discussion



Moreover, the covariance between η and $\hat{\eta}$, due to the normal standard distribution of the two variables, is equal to the correlation coefficient $\rho_{\eta\hat{\eta}}$. Hence, the Eq. (5) can be written as the cross correlation matrix

$$\Sigma_{\eta,\hat{\eta}} = \begin{bmatrix} 1 & \rho_{\eta\hat{\eta}} \\ \rho_{\eta\hat{\eta}} & 1 \end{bmatrix} \quad (6)$$

5 Through the knowledge of the joint and marginal distributions it is easy to compute the predictive distribution according to the Bayes theorem. In fact, the predictive uncertainty, defined as the distribution of the predictand conditioned on the model forecast, can be obtained by calculating the ratio between the joint distribution and the forecast marginal distribution

$$10 \quad f(\eta|\hat{\eta}) = \frac{f(\eta,\hat{\eta})}{f(\hat{\eta})} = \frac{\left[2\pi \begin{vmatrix} 1 & \rho_{\eta\hat{\eta}} \\ \rho_{\eta\hat{\eta}} & 1 \end{vmatrix}\right]^{-\frac{1}{2}} \exp\left(-\frac{1}{2}[\eta \ \hat{\eta}] \begin{bmatrix} 1 & \rho_{\eta\hat{\eta}} \\ \rho_{\eta\hat{\eta}} & 1 \end{bmatrix}^{-1} \begin{bmatrix} \eta \\ \hat{\eta} \end{bmatrix}\right)}{[2\pi]^{-\frac{1}{2}} \exp\left(-\frac{1}{2}\hat{\eta}^2\right)} \quad (7)$$

This equation leads to the definition of the predictive distribution in the normalspace as a normal distribution with moments

$$\begin{aligned} \mu_{\eta|\hat{\eta}} &= \rho_{\eta\hat{\eta}} \cdot \hat{\eta} \\ \sigma_{\eta|\hat{\eta}}^2 &= 1 - \rho_{\eta\hat{\eta}}^2 \end{aligned} \quad (8)$$

15 Therefore, after obtaining the conditional probability in the normal space, the results have to be converted into the real world in order to compute the predictive probability $f(y|\hat{y})$. To do so the predictive density has to be sampled in the normal space and then the obtained quantiles have to be reconverted into the real space by a reverse process. This is due to the fact that the transformation is highly non linear, and, for instance, the mean value in the normal space does not correspond to the mean value in the real world, in fact it corresponds to the median (50% probability) (Todini, 2009). In this process the use of the Weibull plotting position implies the need of using an additional

**Recent developments
in predictive
uncertainty
assessment**

G. Coccia and E. Todini

Title Page

Abstract

Introduction

Conclusions

References

Tables

Figures

⏪

⏩

◀

▶

Back

Close

Full Screen / Esc

Printer-friendly Version

Interactive Discussion



model to be fitted to the tails of all the variables, namely the observations and the model forecast, in the real space, in order to accommodate probability quantiles larger than $\frac{n}{n+1}$ or lower than $\frac{1}{n+1}$.

The multi-model case

5 The previously described MCP methodology has generated the idea of generalizing the procedure using a multi-normal approach (Todini, 2008). Often, a real time forecasting system is composed by more than one model, or a chain of models, and the emergency manager has to take a decision on the basis of multiple forecasts of the same quantity that may also be very different from each other. It is very difficult to find an objective
10 way to state that one model is better than another, or to assign a correct weight to each forecast in order to extrapolate from all the available information a stochastic forecast that allows the emergency to be managed in the best way.

In order to combine several model forecasts, the MCP can be improved by generalizing the bivariate normal approach to a multivariate normal approach (Mardia et al.,
15 1979). In this case the Multivariate space is composed by $M+1$ variables, that are the observed discharges (or water levels) y and the M predictions \hat{y}_k , $k=1, \dots, M$. Using the NQT, all the variables are converted to their transformed values, η and $\hat{\eta}_k$, $k=1, \dots, M$, in the multi-normal space.

All the variables in the normal space have a standard normal distribution and the predictive uncertainty, defined now as the distribution of the future event conditioned
20 on the forecasts of the M models, can be expressed as $(y|\hat{y}_1, \dots, \hat{y}_M)$, for simplicity abbreviated to $f(y|\hat{y}_k)$ for the original variable and $f(\eta|\hat{\eta}_k)$ in the normal space.

The joint distribution is a multi-normal distribution with mean and variance

$$\mu_{\eta, \hat{\eta}_k} = \begin{bmatrix} 0 \\ \vdots \\ 0 \end{bmatrix} \quad (9)$$

Recent developments in predictive uncertainty assessment

G. Coccia and E. Todini

Title Page

Abstract

Introduction

Conclusions

References

Tables

Figures

⏪

⏩

◀

▶

Back

Close

Full Screen / Esc

Printer-friendly Version

Interactive Discussion



$$\Sigma_{\eta, \hat{\eta}_k} = \begin{bmatrix} 1 & \sigma_{\eta \hat{\eta}_1} & \cdots & \sigma_{\eta \hat{\eta}_M} \\ \sigma_{\hat{\eta}_1 \eta} & \ddots & \ddots & \vdots \\ \vdots & \ddots & \ddots & \sigma_{\hat{\eta}_{M-1} \eta} \\ \sigma_{\hat{\eta}_M \eta} & \cdots & \sigma_{\hat{\eta}_M \hat{\eta}_{M-1}} & 1 \end{bmatrix} \quad (10)$$

Moreover, all the covariances, due to the normal standard distribution of all the variables, are equal to the correlation coefficients. So Eq. (10) can be written as the cross correlation matrix

$$\Sigma_{\eta, \hat{\eta}_k} = \begin{bmatrix} 1 & \rho_{\eta \hat{\eta}_1} & \rho_{\eta \hat{\eta}_2} & \cdots & \rho_{\eta \hat{\eta}_M} \\ \rho_{\hat{\eta}_1 \eta} & 1 & \rho_{\hat{\eta}_1 \hat{\eta}_2} & \ddots & \rho_{\hat{\eta}_1 \hat{\eta}_M} \\ \rho_{\hat{\eta}_2 \eta} & \rho_{\hat{\eta}_2 \hat{\eta}_1} & \ddots & \ddots & \vdots \\ \vdots & \ddots & \ddots & \ddots & \rho_{\hat{\eta}_{M-1} \eta} \\ \rho_{\hat{\eta}_M \eta} & \rho_{\hat{\eta}_M \hat{\eta}_1} & \cdots & \rho_{\hat{\eta}_M \hat{\eta}_{M-1}} & 1 \end{bmatrix} \quad (11)$$

Defining

$$\left\{ \begin{array}{l} \Sigma_{\eta \eta} = 1 \\ \Sigma_{\eta \hat{\eta}} = [\rho_{\eta \hat{\eta}_1} \ \rho_{\eta \hat{\eta}_2} \ \cdots \ \rho_{\eta \hat{\eta}_M}] \\ \Sigma_{\hat{\eta} \hat{\eta}} = \begin{bmatrix} 1 & \rho_{\hat{\eta}_1 \hat{\eta}_2} & \cdots & \rho_{\hat{\eta}_1 \hat{\eta}_M} \\ \rho_{\hat{\eta}_2 \hat{\eta}_1} & \ddots & \ddots & \vdots \\ \vdots & \ddots & \ddots & \rho_{\hat{\eta}_{M-1} \hat{\eta}_M} \\ \rho_{\hat{\eta}_M \hat{\eta}_1} & \cdots & \rho_{\hat{\eta}_M \hat{\eta}_{M-1}} & 1 \end{bmatrix} \end{array} \right. \quad (12)$$

Recent developments in predictive uncertainty assessment

G. Coccia and E. Todini

Title Page	
Abstract	Introduction
Conclusions	References
Tables	Figures
◀	▶
◀	▶
Back	Close
Full Screen / Esc	
Printer-friendly Version	
Interactive Discussion	

and substituting Eq. (12) in Eq. (11), the cross correlation matrix can also be written as

$$\Sigma_{\eta, \hat{\eta}_k} = \begin{bmatrix} \Sigma_{\eta\eta} & \Sigma_{\eta\hat{\eta}} \\ \Sigma_{\eta\hat{\eta}}^T & \Sigma_{\hat{\eta}\hat{\eta}} \end{bmatrix} \quad (13)$$

Then the predictive uncertainty can be expressed as

$$f(\eta|\hat{\eta}_k) = \frac{f(\eta, \hat{\eta}_1, \dots, \hat{\eta}_M)}{f(\hat{\eta}_1, \dots, \hat{\eta}_M)} \quad (14)$$

5 The solution of Eq. (14) is easily obtained and leads to a normal distribution with moments derived from Eq. (13) as

$$\mu_{\eta|\hat{\eta}_k} = \Sigma_{\eta\hat{\eta}} \cdot \Sigma_{\hat{\eta}\hat{\eta}}^{-1} \cdot \begin{bmatrix} \hat{\eta}_1 \\ \vdots \\ \hat{\eta}_M \end{bmatrix} \quad (15)$$

$$\sigma_{\eta|\hat{\eta}_k}^2 = 1 - \Sigma_{\eta\hat{\eta}} \cdot \Sigma_{\hat{\eta}\hat{\eta}}^{-1} \cdot \Sigma_{\eta\hat{\eta}}^T$$

Please note that Eq. (15) does not differ from the classical multiple regression results.

10 As done for the univariate case, the predictive uncertainty in the real world, $f(y|\hat{y}_k)$, is obtained by converting $f(\eta|\hat{\eta}_k)$ by means of the inverse NQT.

2.4 The error heteroscedasticity problem: quantile regression and truncated normal joint distributions

15 The latest uncertainty processors (UP) approaches tackle the problem of the heteroscedasticity of the errors often present in hydrological modelling. All the previously described techniques imply homoscedasticity of the error variance, which is assumed to be independent from the magnitude of the observed or forecasted values. In real cases this assumption leads to a lack of accuracy, especially at reproducing high flows,

Recent developments in predictive uncertainty assessment

G. Coccia and E. Todini

Title Page

Abstract

Introduction

Conclusions

References

Tables

Figures

⏪

⏩

◀

▶

Back

Close

Full Screen / Esc

Printer-friendly Version

Interactive Discussion

because the NQT tends to increase the variance of the lower values. Moreover, the number of observed and computed low and medium flows is much larger than that of high flows with the consequence of a higher weight in the determination of the regression or the correlation coefficients used by the different approaches. As a consequence the estimation of high flows in the normal space will be affected by a distortion in the mean as well as an overestimation of the variance, which will inevitably increase when returning into the real space.

Recently, in order to overcome this problem, the quantile regression (Koenker, 2005) was used (Weerts et al., 2010).

2.4.1 Quantile regression

The Quantile Regression (QR) approach tries to represent the error heteroscedasticity identifying a linear variation of the quantiles of the PU as a function of the model forecast magnitude. This technique allows all the desired quantiles of the PU to be assessed in the normal space and then reconverted by means of the inverse NQT to the real space. The τ -th sample quantile is computed solving the Eq. (16), from which is possible to identify the parameters a_τ and b_τ which defines the linear regression for the τ -th quantile.

$$\min_{a_\tau, b_\tau \in R} \sum_{i=1}^n \rho_\tau(\eta - a - b_\tau \cdot \hat{\eta}) \quad (16)$$

where

$$\rho_\tau(x) = \begin{cases} x \cdot (\tau - 1) & \text{if } x < 0 \\ x \cdot \tau & \text{if } x \geq 0 \end{cases}$$

The problem is correctly formulated and allows each quantile of the PU to be computed, but it requires the estimation of at least two parameters per quantile (in the linear case) and the number of parameters to be estimated may become quite large. Moreover, QR not always improves from assuming homoscedasticity: this depends on

Recent developments in predictive uncertainty assessment

G. Coccia and E. Todini

Title Page

Abstract

Introduction

Conclusions

References

Tables

Figures

⏪

⏩

◀

▶

Back

Close

Full Screen / Esc

Printer-friendly Version

Interactive Discussion



the actual distribution of the errors. Figure 3a and b show two situations in which the use of QR leads to very different results. Figure 3a is an optimal situation for using QR because the variation of error variance is linearly decreasing with the magnitude of the forecasts and the resulting quantiles well represent the real distribution of the data. On the contrary, in Fig. 3b it is not possible to identify a linear variation of the error variance and the use QR does not provide improved assessments of PU, particularly for high forecast values.

2.4.2 Truncated normal joint distributions

In the situation represented in Fig. 3b a different alternative approach can be used to improve results. Namely, within the MCP framework the entire normal domain is divided into two (or more) sub-domains where Truncated Normal Distributions (TNDs) can be used (Coccia and Todini, 2010). In this case, the MCP can be applied assuming that the joint distribution in the normal space is not unique, but can be divided into two (or more) TNDs. A threshold separating low flows from high flows in the forecast domain is relatively easy to be identified. Figure 4 shows the two TNDs that can be used in the example.

The identification of the two TNDs is not immediate, but can be obtained by the following procedure that depends on the number of available forecasting models.

2.4.3 TNDs with only one forecasting model

After converting the original variables y and \hat{y} to their transformed values η and $\hat{\eta}$, the so obtained samples are assumed to belong to two unknown normal distributions truncated over $\hat{\eta}$ by a threshold a . The moments of these truncated distributions can be estimated by equating them to the sampling moments.

Recent developments in predictive uncertainty assessment

G. Coccia and E. Todini

Title Page

Abstract

Introduction

Conclusions

References

Tables

Figures

⏪

⏩

◀

▶

Back

Close

Full Screen / Esc

Printer-friendly Version

Interactive Discussion



For the sample that includes the high flows, the truncated normal distribution for $\hat{\eta} > a$ is

$$f(\hat{\eta}|\hat{\eta} > a) = \frac{f(\hat{\eta})}{\int_a^{+\infty} f(\hat{\eta})d\hat{\eta}} = \frac{f(\hat{\eta})}{1 - F_{\hat{\eta}}(a)} \quad (17)$$

with $f(\hat{\eta})$ defined as

$$f(\hat{\eta}) = \frac{1}{\sqrt{2\pi}s_{\hat{\eta}}} \exp\left\{-\frac{1}{2}\left(\frac{\hat{\eta} - m_{\hat{\eta}}}{s_{\hat{\eta}}}\right)^2\right\} \quad (18)$$

where \hat{m} and \hat{s} are the mean and the standard deviation of the non truncated, albeit unknown distribution.

Therefore, the joint distribution is the following truncated normal bivariate distribution

$$f(\eta, \hat{\eta}|\hat{\eta} > a) = \frac{f(\eta, \hat{\eta})}{\int_{-\infty}^{+\infty} [\int_a^{+\infty} f(\eta, \hat{\eta})d\hat{\eta}] d\eta} = \frac{f(\eta, \hat{\eta})}{1 - F_{\hat{\eta}}(a)} \quad (19)$$

Where $f(\eta, \hat{\eta})$ is defined as

$$f(\eta, \hat{\eta}) = \frac{\exp\left\{-\frac{1}{2}[\eta - m_{\eta} \quad \hat{\eta} - m_{\hat{\eta}}] \mathbf{S}^{-1} \begin{bmatrix} \eta - m_{\eta} \\ \hat{\eta} - m_{\hat{\eta}} \end{bmatrix}\right\}}{\sqrt{2\pi|\mathbf{S}|}} \quad (20)$$

$$\text{where } \mathbf{S} = \begin{bmatrix} s_{\hat{\eta}}^2 & s_{\eta\hat{\eta}} \\ s_{\eta\hat{\eta}} & s_{\eta}^2 \end{bmatrix}.$$

In Eqs. (18) and (20), the values of $m_{\hat{\eta}}$, $s_{\hat{\eta}}$, m_{η} , s_{η} and $s_{\eta\hat{\eta}}$ are unknown but can be derived from the sampling moments. Applying the Bayes theorem to the truncated normal, the predictive uncertainty (which in this case represents the probability distribution of η conditional on the model forecast $\hat{\eta}^* > a$) becomes

$$f(\eta|\hat{\eta} > a, \hat{\eta}^*) = \frac{f(\eta, \hat{\eta}|\hat{\eta} > a, \hat{\eta}^*)}{f(\hat{\eta}|\hat{\eta} > a, \hat{\eta}^*)} = \frac{f(\eta, \hat{\eta}|\hat{\eta}^*)}{f(\hat{\eta}|\hat{\eta}^*)} \quad (21)$$

**Recent developments
in predictive
uncertainty
assessment**

G. Coccia and E. Todini

Title Page

Abstract

Introduction

Conclusions

References

Tables

Figures

⏪

⏩

◀

▶

Back

Close

Full Screen / Esc

Printer-friendly Version

Interactive Discussion



and it is normally distributed with mean and variance

$$\mu_{\eta|\hat{\eta}>a,\hat{\eta}^*} = m_{\eta} + \frac{s_{\eta\hat{\eta}}}{s_{\hat{\eta}}^2}(\hat{\eta}^* - m_{\hat{\eta}})$$

$$\sigma_{\eta|\hat{\eta}>a,\hat{\eta}^*}^2 = s_{\eta}^2 - \frac{s_{\eta\hat{\eta}}^2}{s_{\hat{\eta}}^2} \quad (22)$$

Similarly for $\hat{\eta}^* < a$, Eqs. (17) and (19) become, respectively

$$f(\hat{\eta}|\hat{\eta} < a, \hat{\eta}^*) = \frac{f(\hat{\eta})}{\int_{-\infty}^a f(\hat{\eta})d\hat{\eta}} = \frac{f(\hat{\eta})}{F_{\hat{\eta}}(a)} \quad (23)$$

$$f(\eta, \hat{\eta}|\hat{\eta} < a, \hat{\eta}^*) = \frac{f(\eta, \hat{\eta})}{\int_{-\infty}^{+\infty} [\int_{-\infty}^a f(\eta, \hat{\eta})d\hat{\eta}] d\eta} = \frac{f(\eta, \hat{\eta})}{F_{\hat{\eta}}(a)} \quad (24)$$

According to the procedure described in Appendix A, the previous equations allow the PU in the normal space to be defined as a normal distribution with mean and variance

$$\mu_{\eta|\hat{\eta}>a,\hat{\eta}^*} = \mu_{\eta} + \frac{\sigma_{\eta\hat{\eta}}}{\sigma_{\hat{\eta}}^2}(\hat{\eta}^* - \mu_{\hat{\eta}})$$

$$\sigma_{\eta|\hat{\eta}>a,\hat{\eta}^*}^2 = \sigma_{\eta}^2 - \frac{\sigma_{\eta\hat{\eta}}^2}{\sigma_{\hat{\eta}}^2} \quad (25)$$

for the case that the predicted value $\hat{\eta}^*$ is greater than the threshold value a . Here μ_{η} , $\mu_{\hat{\eta}}$ are, respectively the sample means of $\eta|\hat{\eta}>a$ and $\hat{\eta}|\hat{\eta}>a$ and σ_{η} , $\sigma_{\hat{\eta}}$ are their sample standard deviations. These moments are obviously computed considering only the sample including the data belong to the upper sample.

**Recent developments
in predictive
uncertainty
assessment**

G. Coccia and E. Todini

Title Page	
Abstract	Introduction
Conclusions	References
Tables	Figures
◀	▶
◀	▶
Back	Close
Full Screen / Esc	
Printer-friendly Version	
Interactive Discussion	



If $\hat{\eta}^*$ is lower than the threshold value a , the mean and variance of PU in normal space are

$$\begin{aligned}\mu_{\eta|\hat{\eta}, \hat{\eta}^* < a} &= \mu_{\eta} + \frac{\sigma_{\eta\hat{\eta}}}{\sigma_{\hat{\eta}}^2} (\hat{\eta}^* - \mu_{\hat{\eta}}) \\ \sigma_{\eta|\hat{\eta}, \hat{\eta}^* < a}^2 &= \sigma_{\eta}^2 - \frac{\sigma_{\eta\hat{\eta}}^2}{\sigma_{\hat{\eta}}^2}\end{aligned}\tag{26}$$

where μ_{η} , $\mu_{\hat{\eta}}$, σ_{η} and $\sigma_{\hat{\eta}}$ are computed taking in account only the data of the lower sample.

2.4.4 TNDs with more than one forecasting model

When dealing with more than one model, the procedure becomes a bit more difficult. The threshold should be identified for each model and the joint distribution would be represented by 2^M MTNDs (where M is the number of models) that include all the possible simultaneous combinations of each model overtopping or not its respective threshold. The moments of each MTNDs should be obtained by means of the sampling moments computation, but unfortunately in real cases often the available data are not enough to identify representative samples and the MTNDs cannot be well assessed.

In order to avoid this situation the problem can be tackled with a different approach. The MCP can be applied in three phases. Firstly, each model is processed separately using the TNDs as described above. In this phase, for each model its threshold is identified. In the second phase, the series of expected values of each model simulation (previously obtained) are combined using two MTNDs identified on the basis of the model that better represented the high flows. In other words, for each model the variances of the upper sample are computed and then they are compared each other in order to identify which model will be used in the second phase in order to split the multivariate joint distribution in two MTNDs. Finally, in the third phase the series

Recent developments in predictive uncertainty assessment

G. Coccia and E. Todini

Title Page	
Abstract	Introduction
Conclusions	References
Tables	Figures
⏪	⏩
◀	▶
Back	Close
Full Screen / Esc	
Printer-friendly Version	
Interactive Discussion	



of expected values computed in the second phase is processed using the TNDs as described above. The detailed description of the procedure is the following.

Considering M available models and applying to each model the methodology described in Sect. 2.4.2.1, the following parameters are computed

- 5 – a'_i = threshold used for identifying the TNDs of the model $i=1, M$
- $\sigma_{\eta|\hat{\eta}_i > \hat{\eta}_i^* > a'_i}^2$ = conditioned variance of the upper TND for model $i=1, M$

In the second phase the joint MTNDs are identified on the basis of the model k , which is the model that better represents the high flows:

$$\sigma_{\eta|\hat{\eta}_k > a'_k, \hat{\eta}_k^*}^2 < \sigma_{\eta|\hat{\eta}_i > a'_i, \hat{\eta}_i^*}^2 \quad \forall i \neq k$$

10 Considering the upper sample, for sake of simplicity let's define the vector \mathbf{a} , such as

$$\begin{cases} a_i = -\infty & \forall i \neq k \\ a_k = a'_k \end{cases}$$

the vector $\hat{\boldsymbol{\eta}}$ represents the variables related to the model simulations,

$$\hat{\boldsymbol{\eta}} = \begin{bmatrix} \hat{\eta}_1 \\ \vdots \\ \hat{\eta}_M \end{bmatrix}.$$

The joint distribution of the simulated variables $\hat{\eta}_i > -\infty \quad \forall i \neq k$ and $\hat{\eta}_k > a_k$ is

$$15 \quad f(\hat{\boldsymbol{\eta}}|\hat{\eta}_k > a_k) = \frac{f(\hat{\boldsymbol{\eta}})}{1 - F_{\hat{\eta}_k}(a_k)} \quad (27)$$

Where $f(\hat{\boldsymbol{\eta}})$ is defined as

$$f(\hat{\boldsymbol{\eta}}) = \frac{\exp\left\{-\frac{1}{2}[\hat{\boldsymbol{\eta}} - \hat{\mathbf{m}}]S_{\hat{\boldsymbol{\eta}}\hat{\boldsymbol{\eta}}}^{-1}[\hat{\boldsymbol{\eta}} - \hat{\mathbf{m}}]^T\right\}}{(2\pi)^{1/M} \sqrt{|\mathbf{S}_{\hat{\boldsymbol{\eta}}\hat{\boldsymbol{\eta}}}|}} \quad (28)$$

Recent developments in predictive uncertainty assessment

G. Coccia and E. Todini

Title Page	
Abstract	Introduction
Conclusions	References
Tables	Figures
◀	▶
◀	▶
Back	Close
Full Screen / Esc	
Printer-friendly Version	
Interactive Discussion	



where

$$\hat{m} = \begin{bmatrix} m_{\hat{\eta}_1} \\ \vdots \\ m_{\hat{\eta}_M} \end{bmatrix}$$

is the vector containing the means of the marginal distributions of $\hat{\eta}$ and $\mathbf{S}_{\hat{\eta}\hat{\eta}}$ is the covariance matrix between the variables $\hat{\eta}$

$$\mathbf{S}_{\hat{\eta}\hat{\eta}} = \begin{bmatrix} s_{\hat{\eta}_1}^2 & s_{\hat{\eta}_2\hat{\eta}_1} & \cdots & s_{\hat{\eta}_M\hat{\eta}_1} \\ s_{\hat{\eta}_1\hat{\eta}_2} & \ddots & \ddots & \vdots \\ \vdots & \ddots & \ddots & s_{\hat{\eta}_{M-1}\hat{\eta}_1} \\ s_{\hat{\eta}_1\hat{\eta}_M} & \cdots & s_{\hat{\eta}_1\hat{\eta}_{M-1}} & s_{\hat{\eta}_M}^2 \end{bmatrix} \quad (29)$$

Therefore, the joint distribution of all the variables is the following MTND

$$f(\eta, \hat{\eta} | \hat{\eta}_k > a_k) = \frac{f(\eta, \hat{\eta})}{1 - F_{\hat{\eta}_k}(a_k)} \quad (30)$$

Where $f(\eta, \hat{\eta})$ is defined as

$$f(\eta, \hat{\eta}) = \frac{\exp\left\{-\frac{1}{2} [\eta - m \hat{\eta} - \hat{m}] \mathbf{S}^{-1} \begin{bmatrix} \eta - m \\ \hat{\eta} - \hat{m} \end{bmatrix}\right\}}{(2\pi)^{\frac{1}{M+1}} \cdot \sqrt{|\mathbf{S}|}} \quad (31)$$

where m is the mean of the marginal distributions of η and

$$\mathbf{S} = \begin{bmatrix} S_{\eta\eta} & S_{\eta\hat{\eta}} \\ S_{\eta\hat{\eta}}^T & \mathbf{S}_{\hat{\eta}\hat{\eta}} \end{bmatrix} \quad (32)$$

Recent developments in predictive uncertainty assessment

G. Coccia and E. Todini

Title Page

Abstract

Introduction

Conclusions

References

Tables

Figures

◀

▶

◀

▶

Back

Close

Full Screen / Esc

Printer-friendly Version

Interactive Discussion

with:

$$S_{\eta\eta} = s_{\eta}^2$$

$$S_{\eta\hat{\eta}} = [s_{\eta\hat{\eta}_1} \dots s_{\eta\hat{\eta}_m}]$$

In Eqs. (28) and (31), \hat{m} , $S_{\hat{\eta}\hat{\eta}}$, m , $S_{\eta\eta}$ and $S_{\eta\hat{\eta}}$ are unknown but can be derived from the sampling moments.

Applying the Bayes theorem to the joint MTND, the predictive uncertainty, namely the probability distribution of η conditional on the realization of the model forecasts $\hat{\eta}^*$, becomes

$$f(\eta|\hat{\eta}_k > a_k, \hat{\eta}^*) = \frac{f(\eta, \hat{\eta}|\hat{\eta}_k > a_k, \hat{\eta}^*)}{f(\hat{\eta}|\hat{\eta}_k > a_k, \hat{\eta}^*)} = \frac{f(\eta, \hat{\eta}|\hat{\eta}^*)}{f(\hat{\eta}|\hat{\eta}^*)} \quad (33)$$

Please, note that Eq. (33) is conceptually equal to Eq. (19). In other words, being M the number of models considered, $f(\eta, \hat{\eta})$ is a $(M+1)$ -variate and $f(\hat{\eta})$ is M -variate, and in Eq. (19) $M=1$.

The conditional distribution of Eq. (33) is normally distributed with mean and variance

$$\mu_{\eta|\hat{\eta}_k > a_k, \hat{\eta}^*} = m + S_{\eta\hat{\eta}} \cdot S_{\hat{\eta}\hat{\eta}}^{-1} \cdot (\hat{\eta}^* - \hat{m})$$

$$\sigma_{\eta|\hat{\eta}_k > a_k, \hat{\eta}^*}^2 = S_{\eta\eta} - S_{\eta\hat{\eta}} \cdot S_{\hat{\eta}\hat{\eta}}^{-1} \cdot S_{\eta\hat{\eta}}^T \quad (34)$$

Following the procedure described in Appendix A, the previous equations lead to define PU in the normal space as a normal distribution with mean and variance

$$\mu_{\eta|\hat{\eta}_k > a_k, \hat{\eta}^*} = \mu + \Sigma_{\eta\hat{\eta}} \cdot \Sigma_{\hat{\eta}\hat{\eta}}^{-1} \cdot (\hat{\eta}^* - \hat{\mu})$$

$$\sigma_{\eta|\hat{\eta}_k > a_k, \hat{\eta}^*}^2 = \Sigma_{\eta\eta} - \Sigma_{\eta\hat{\eta}} \cdot \Sigma_{\hat{\eta}\hat{\eta}}^{-1} \cdot \Sigma_{\eta\hat{\eta}}^T \quad (35)$$

if the predicted value of the model k , $\hat{\eta}_k^*$, is greater than the threshold value a_k . Here μ and $\hat{\mu}$ are, respectively the sample means of $\eta|\hat{\eta}_k > a_k$ and $\hat{\eta}|\hat{\eta}_k > a_k$ and $\Sigma_{\eta\eta}$, $\Sigma_{\eta\hat{\eta}}$, $\Sigma_{\hat{\eta}\hat{\eta}}$ are the components of the covariance matrix of $\eta, \hat{\eta}|\hat{\eta}_k > a_k$.

Recent developments
in predictive
uncertainty
assessment

G. Coccia and E. Todini

Title Page

Abstract

Introduction

Conclusions

References

Tables

Figures

⏪

⏩

◀

▶

Back

Close

Full Screen / Esc

Printer-friendly Version

Interactive Discussion



Similarly for the sample below the threshold and taking into account that the vector \mathbf{a} is defined as:

$$\begin{cases} a_i = +\infty & \forall i \neq k \\ a_k = a'_k \end{cases}$$

Equations (27) and (30) become, respectively

$$5 \quad f(\hat{\boldsymbol{\eta}} | \hat{\eta}_k < a_k) = \frac{f(\hat{\boldsymbol{\eta}})}{F_{\hat{\eta}_k}(a_k)} \quad (36)$$

$$f(\eta, \hat{\boldsymbol{\eta}} | \hat{\eta}_k < a_k) = \frac{f(\eta, \hat{\boldsymbol{\eta}})}{F_{\hat{\eta}_k}(a_k)} \quad (37)$$

Hence, if $\hat{\eta}_k^*$ is lower than the threshold value a_k , the mean and variance of PU in normal space are

$$\begin{aligned} \mu_{\eta | \hat{\eta}_k < a_k, \hat{\boldsymbol{\eta}}^*} &= \boldsymbol{\mu} + \boldsymbol{\Sigma}_{\eta \hat{\boldsymbol{\eta}}} \cdot \boldsymbol{\Sigma}_{\hat{\boldsymbol{\eta}} \hat{\boldsymbol{\eta}}}^{-1} \cdot (\hat{\boldsymbol{\eta}}^* - \hat{\boldsymbol{\mu}}) \\ \sigma_{\eta | \hat{\eta}_k < a_k, \hat{\boldsymbol{\eta}}^*}^2 &= \Sigma_{\eta \eta} - \boldsymbol{\Sigma}_{\eta \hat{\boldsymbol{\eta}}} \cdot \boldsymbol{\Sigma}_{\hat{\boldsymbol{\eta}} \hat{\boldsymbol{\eta}}}^{-1} \cdot \boldsymbol{\Sigma}_{\eta \hat{\boldsymbol{\eta}}}^T \end{aligned} \quad (38)$$

10 where $\boldsymbol{\mu}$, $\hat{\boldsymbol{\mu}}$, $\Sigma_{\eta \eta}$, $\boldsymbol{\Sigma}_{\eta \hat{\boldsymbol{\eta}}}$ and $\boldsymbol{\Sigma}_{\hat{\boldsymbol{\eta}} \hat{\boldsymbol{\eta}}}$ are computed taking in account only the data of the lower sample.

3 Examples of application

The examples reported in this paper aim at showing the benefits of using a multi-model approach, which is possible when using the proposed methodology.

15 3.1 Case study and available data

The NOAA's National Weather Service, has provided a long series of observed discharge and precipitation data for the Baron Fork River, OK, USA within the frame of

Recent developments in predictive uncertainty assessment

G. Coccia and E. Todini

Title Page

Abstract

Introduction

Conclusions

References

Tables

Figures

⏪

⏩

◀

▶

Back

Close

Full Screen / Esc

Printer-friendly Version

Interactive Discussion

the DMIP 2 Project which aims at comparing distributed hydrological models. Using this data set three models were developed: two physically based hydrological models, the TOPKAPI model (Todini and Ciarapica, 2001; Liu and Todini, 2002) and TETIS model (Frances et al., 2007; Velez et al., 2009), and an additional data driven model based on Artificial Neural Networks. The catchment has a drainage area of about 800 km² at the measurement station of Eldon with a mean slope around 0.25%, while some kilometres downstream Eldon the river flows into the Illinois river. The simulations provided by the three models have been processed using the MCP firstly separately and then combined each other.

Available meteorological data were hourly rain and temperature grids included between 1 October 1995 and 30 September 2002, with a 4 km resolution. During the same period the observed discharges in the measurement station of Eldon, OK, were available, too. Summarizing, the available data allow the basin behaviour to be simulated during a long period of about 7 years with a time step of 1 h.

3.2 The real time flood forecasting models

The TOPKAPI model has been developed at the University of Bologna (Todini and Ciarapica, 2001; Liu and Todini, 2002), it is composed of six components, which take into account the surface, sub-surface and deep flows, the routing in the channel, the snow accumulation/melt and the evapotranspiration. The application domain is divided in cells where the mass and momentum balance are solved at every time step. The model has been calibrated by a trial and error procedure applied to the data included between 1 October 1996 and 30 September 2002; the year included between 1 October 1995 and 30 September 1996 has been used as “warm up” period, allowing the model to reach a reasonable initial state.

In the TETIS model, developed by the Polytechnic University of Valencia (Frances et al., 2007; Velez et al., 2009), the conceptual scheme, at each cell, consists of a series of 5 connected tanks, each one of them representing different water storages in

**Recent developments
in predictive
uncertainty
assessment**

G. Coccia and E. Todini

Title Page

Abstract Introduction

Conclusions References

Tables Figures

⏪ ⏩

◀ ▶

Back Close

Full Screen / Esc

Printer-friendly Version

Interactive Discussion



the soil column. The vertical connections between tanks describe the precipitation, evapotranspiration, infiltration and percolation processes, whereas, the horizontal flows represent the main hydrological processes as: snowmelt, overland runoff, interflow and base flow. The routing along the channel network couples its geomorphologic characteristics with the kinematic wave approach. The Tetis model has an automatic calibration procedure applied to the hydrological year included between October 2000 and September 2001. As done for the TOPKAPI model, the first year of data has been used as “warm up” period and with the remaining data the model has been validated.

The Artificial Neural Network model is composed of two main phases. Firstly the data are divided in three groups by means of a Self Organizing Map (SOM) network that allows the data to be automatically classified. (Kohonen, 1990; Pujol, 2009). If the time at which the prediction is done is called t_0 , the input data to the SOM network are the accumulated precipitation of 2 days before t_0 , the discharge observed at t_0 and the gradient of the discharge during 2 h before t_0 . The SOM network has been calibrated using the data included between 1 October 1995 and 31 May 1997, the remaining data until 30 September 2002 have been used for the validation. The three sets of data obtained by the automatic classification have been used separately in order to calibrate three different Multi Layer Perceptron (MLP) networks (Werbos, 1974; Parker, 1987; Werbos, 1988, 1990; Pujol, 2009), which input data are the observed precipitation during 13 h before t_0 and the observed discharges during 3 h before t_0 . The output of the networks is the discharge 6 h after the t_0 . Summarizing, the data have been divided in three groups using the SOM, in order to identify three different hydrological states of the system, and each group has been calibrated with a Feed Forward Network in order to forecast the discharge 6 h in advance. Moreover, to avoid the risk of overfitting the calibration data, the *early stopping procedure* has been used introducing a verification set of data, included between 1 June 1997 and 31 January 1998. The data included between 1 February 1998 and 30 September 2002 have been used for validating the model.

**Recent developments
in predictive
uncertainty
assessment**G. Coccia and E. Todini

[Title Page](#)[Abstract](#)[Introduction](#)[Conclusions](#)[References](#)[Tables](#)[Figures](#)[⏪](#)[⏩](#)[◀](#)[▶](#)[Back](#)[Close](#)[Full Screen / Esc](#)[Printer-friendly Version](#)[Interactive Discussion](#)

In order to make congruent the forecasts of each model also the TETIS and TOP-KAPI models have been used to predict the discharge 6 h in advance, assuming, as done with the ANN, that precipitation is null during the forecast time.

In Fig. 6 a schematic summary of the division of the data used for calibrating and validating each model is depicted.

The two physically based models are conceptually quite similar; it can be highlighted that the Topkapi model tends to underestimate the highest flood events, to overestimate the smallest ones and to reproduce the flood events of medium magnitude quite well. The Tetis model also generally underestimates the highest events and often underestimates the small events too. The ANN model, due to its nature of data driven model, is not able to well reproduce the pick flows, which are often underestimated and predicted with late of 1 or 2 h, but it has a perfect behaviour in reproducing the low flows.

3.3 Predictive uncertainty assessment

The MCP has been applied in three phases and in every phase the Joint TNDs have been used.

Firstly the models simulations have been processed separately. All the historical data have been processed and the expected value of the predictive distribution has been computed at each time step. In the second phase, the series of the expected values of each model simulation have been processed with the MCP multivariate approach and the combined expected value has been computed from the predictive uncertainty of each time step. Finally, in the third phase, this series of expected values has been processed.

Figure 7a and b summarize the obtained results with regard to the models combination computed by means of the expected value of the predictive distribution. Figure 7a represents the error standard deviation and Fig. 7b represents the Nash-Sutcliffe coefficient.

Recent developments in predictive uncertainty assessment

G. Coccia and E. Todini

Title Page

Abstract

Introduction

Conclusions

References

Tables

Figures

⏪

⏩

◀

▶

Back

Close

Full Screen / Esc

Printer-friendly Version

Interactive Discussion



threshold when the expected value of prediction equals $250 \text{ m}^3 \text{ s}^{-1}$, computed for each model and their Bayesian combination. One can see the reduction of exceedance probability as a function of the quality of the forecast. Finally, the effect of the introduction of the new probabilistic forecast paradigm can be appreciated in Table 2 where, similarly to what is qualitatively displayed in Fig. 2, the expected value of the prediction corresponding to the probability of 20% that the true value will exceed the $350 \text{ m}^3 \text{ s}^{-1}$ threshold, computed for each model and their Bayesian combination. As can be seen better models allow to wait until the expected value of prediction is closer to the flooding level, while worse models require earlier action corresponding to lower levels on the basis of the principle of precaution, which corresponds to the fact that the decision maker is more uncertain.

5 Conclusions

The large availability of data on the Baron Fork River allowed the Tetis and Topkapi hydrologic models and an Artificial Neural Network model to be applied with good results in terms of forecast quality, and the MCP to be tested with special regard to the multivariate methodology. In particular, it has been possible to highlight some important issues such as the improvement of the forecast quality, the assessment of the predictive uncertainty and the computation of the probability of exceeding a flooding alert threshold.

The combination of the three models' predictions, obtained by assigning different weights to each model according to the Bayesian theory, allows the forecast quality to be improved as shown by the evaluation indexes in Fig. 7a and b. The two physically based model structures are very similar, so this leads to a little gain in terms of forecast improvement, represented by the standard deviation of the errors and the Nash-Sutcliffe efficiency index (Fig. 7a and b). On the contrary, the combination of one physically based model with the data driven model leads to greater improvements in forecast and, in particular, the combination of all the three models gives the best values

Recent developments in predictive uncertainty assessment

G. Coccia and E. Todini

Title Page

Abstract

Introduction

Conclusions

References

Tables

Figures

⏪

⏩

◀

▶

Back

Close

Full Screen / Esc

Printer-friendly Version

Interactive Discussion



of the analyzed indexes (Fig. 7a and b). These results show that the combination of models of different nature allows the probabilistic forecast to improve the deterministic forecast of each model, taking advantage of the benefits of different hydrological approaches. The MCP has proved to be quite effective at converting the models *virtual reality* into the uncertainty of the future real event by computing its probability distribution. It is interesting to note that during the validation period, the percentage of the observed data that fall outside the 90% MCP uncertainty band is 10.3% (7.3% below the lower quantile and 3% above the upper one). This means that the uncertainty band can be considered satisfactorily estimated also during validation period, even if the percentage of data above the upper quantile is slightly greater than the one below the lower quantile. Moreover, it is very important to note that the MCP leads to obtain an objective forecast from the output of several models and can give important support in taking a decision based on various and different forecasts.

Finally, the assessment of the predictive uncertainty also allows the probability of exceeding an alert level to be estimated. With this work, a discussion about the convenience of using a probability threshold instead of a deterministic one in order to estimate the flooding risk and help the decision making process about giving or not a flood alarm, has been initiated. In fact, the paper highlighted the need for a change in flood forecasting and warning paradigm which should go through the definition of *probabilistic threshold* with the aim of take advantage in a more effective way of the use of probabilistic forecasts. The results presented in Sect. 4 show the correctness of the methodology in estimating the probability of exceeding the alarm threshold. When the hydrological forecast issue can be defined in terms of a binary response (giving or not a flood alarm) the probabilistic threshold concept allows the reliability and the knowledge provided by different models to be taken in account. Therefore, the emergency manager can express his/her propensity to the risk in terms of probability of flooding and not just comparing a pre-fixed real threshold with the virtual reality of the model forecast, as usually done with a deterministic approach.

Recent developments in predictive uncertainty assessment

G. Coccia and E. Todini

[Title Page](#)[Abstract](#)[Introduction](#)[Conclusions](#)[References](#)[Tables](#)[Figures](#)[Back](#)[Close](#)[Full Screen / Esc](#)[Printer-friendly Version](#)[Interactive Discussion](#)

Appendix A

Considering M available forecasting models and starting from the hypothesis that the data divided over $\hat{\eta}_k$ by the threshold a_k , belong to two Multivariate Truncated Normal Distributions (MTNDs) and considering the upper sample, the marginal distributions of $\eta|\hat{\eta}_k > a_k$ and $\hat{\eta}|\hat{\eta}_k > a_k$ are, respectively a Truncated Normal (TN) and a Multivariate Truncated Normal (MTN) called

$$f(\eta|\hat{\eta}_k > a_k) = TN(\mu, \Sigma_{\eta\eta}) \quad (A1)$$

and

$$f(\hat{\eta}|\hat{\eta}_k > a_k) = MTN(\hat{\mu}, \Sigma_{\hat{\eta}\hat{\eta}}) \quad (A2)$$

10 Their Joint Truncated Distribution is called

$$f(\eta, \hat{\eta}|\hat{\eta}_k > a_k) = MTN\left(\begin{bmatrix} \mu \\ \hat{\mu} \end{bmatrix}, \begin{bmatrix} \Sigma_{\eta\eta} & \Sigma_{\eta\hat{\eta}} \\ \Sigma_{\hat{\eta}\eta} & \Sigma_{\hat{\eta}\hat{\eta}} \end{bmatrix}\right) \quad (A3)$$

All the parameters μ , $\Sigma_{\eta\eta}$, $\hat{\mu}$, $\Sigma_{\hat{\eta}\hat{\eta}}$ and $\Sigma_{\eta\hat{\eta}}$ are known, because they are assumed to be equal to the sample ones.

The distributions

$$15 f(\eta) = N(m, S_{\eta\eta}) \quad (A4)$$

$$f(\hat{\eta}) = N(\hat{m}, S_{\hat{\eta}\hat{\eta}}) \quad (A5)$$

$$f(\eta, \hat{\eta}) = N\left(\begin{bmatrix} m \\ \hat{m} \end{bmatrix}, \begin{bmatrix} S_{\eta\eta} & S_{\eta\hat{\eta}} \\ S_{\hat{\eta}\eta} & S_{\hat{\eta}\hat{\eta}} \end{bmatrix}\right) \quad (A6)$$

are the Multivariate Complete Normal Distributions (MCNDs) to which the MTNDs, respectively represented by Eqs. (A1), (A2), (A3), are supposed to belong.

20 All the parameters of the MCNDs, m , $S_{\eta\eta}$, \hat{m} , $S_{\hat{\eta}\hat{\eta}}$ and $S_{\eta\hat{\eta}}$, are unknown and they must be identified in order to define the conditioned distribution, that is the PU in the

normal space conditioned to the model forecasts that transformed using the NQT gives a value for the model k greater than the threshold value a_k .

In fact, as described by Eq. (33), the conditioned distribution is

$$f(\eta|\hat{\eta}_k > a_k, \hat{\eta}^*) = \frac{f(\eta, \hat{\eta})}{f(\hat{\eta})} = N\left(\mu_{\eta|\hat{\eta}_k > a_k, \hat{\eta}^*}, \sigma_{\eta|\hat{\eta}_k > a_k, \hat{\eta}^*}^2\right) \quad (\text{A7})$$

Hence, the mean and variance of the conditioned distribution are (see Eq. 34)

$$\mu_{\eta|\hat{\eta}_k > a_k, \hat{\eta}^*} = m + \mathbf{S}_{\eta\hat{\eta}} \cdot \mathbf{S}_{\hat{\eta}\hat{\eta}}^{-1} \cdot (\hat{\eta}^* - \hat{m}) \quad (\text{A8})$$

$$\sigma_{\eta|\hat{\eta}_k > a_k, \hat{\eta}^*}^2 = S_{\eta\eta} - \mathbf{S}_{\eta\hat{\eta}} \cdot \mathbf{S}_{\hat{\eta}\hat{\eta}}^{-1} \cdot \mathbf{S}_{\eta\hat{\eta}}^T \quad (\text{A9})$$

The parameters of the MCNDs can be derived from the following equations, provided by the truncated multi-normal distribution theory (Tallis, 1961), which relate the moments of the MTNDs to the ones of the MCNDs.

$$m = \mu - \frac{\sigma_{\eta\hat{\eta}_k}}{\sqrt{\sigma_{\hat{\eta}_k\hat{\eta}_k}}} \cdot \lambda(\alpha_k) \quad (\text{A10})$$

$$\hat{m} = \hat{\mu} - \frac{\boldsymbol{\Sigma}_{\hat{\eta}\hat{\eta}_k}}{\sqrt{\sigma_{\hat{\eta}_k\hat{\eta}_k}}} \cdot \lambda(\alpha_k) \quad (\text{A11})$$

$$S_{\eta\eta} = \sigma_{\eta\eta} + \frac{\sigma_{\eta\hat{\eta}_k}^2}{\sigma_{\hat{\eta}_k\hat{\eta}_k}} \cdot \delta(\alpha_k) \quad (\text{A12})$$

$$\mathbf{S}_{\hat{\eta}\hat{\eta}} = \boldsymbol{\Sigma}_{\hat{\eta}\hat{\eta}} + \frac{\boldsymbol{\Sigma}_{\hat{\eta}\hat{\eta}_k} \cdot \boldsymbol{\Sigma}_{\hat{\eta}\hat{\eta}_k}^T}{\sigma_{\hat{\eta}_k\hat{\eta}_k}} \cdot \delta(\alpha_k) \quad (\text{A13})$$

$$\mathbf{S}_{\eta\hat{\eta}} = \boldsymbol{\Sigma}_{\eta\hat{\eta}} + \frac{\sigma_{\eta\hat{\eta}_k} \cdot \boldsymbol{\Sigma}_{\hat{\eta}\hat{\eta}_k}}{\sigma_{\hat{\eta}_k\hat{\eta}_k}} \cdot \delta(\alpha_k) \quad (\text{A14})$$

**Recent developments
in predictive
uncertainty
assessment**

G. Coccia and E. Todini

Title Page

Abstract

Introduction

Conclusions

References

Tables

Figures

⏪

⏩

◀

▶

Back

Close

Full Screen / Esc

Printer-friendly Version

Interactive Discussion



where

$$\alpha_k = \frac{a_k - m_k}{\sqrt{S_{\hat{\eta}_k \hat{\eta}_k}}}$$

$$\lambda(\alpha_k) = \frac{\phi(\alpha_k)}{1 - \Phi(\alpha_k)} \quad (A15)$$

$$\delta(\alpha_k) = \lambda(\alpha_k) \cdot [\lambda(\alpha_k) - \alpha_k]$$

5 and ϕ and Φ , respectively represent the pdf and the cdf of the normal standard distribution.

The equality between Eq. (34) and Eq. (35) (or between Eq. 22 and Eq. 25 for the bi-dimensional case), leads to

$$\mu_{\eta|\hat{\eta}_k > a_k, \hat{\eta}^*} = m + S_{\eta \hat{\eta}} \cdot S_{\hat{\eta} \hat{\eta}}^{-1} \cdot (\hat{\eta}^* - \hat{m}) = \mu + \Sigma_{\eta \hat{\eta}} \cdot \Sigma_{\hat{\eta} \hat{\eta}}^{-1} \cdot (\hat{\eta}^* - \hat{\mu}) \quad (A16)$$

$$\sigma_{\eta|\hat{\eta}_k > a_k, \hat{\eta}^*}^2 = S_{\eta \eta} - S_{\eta \hat{\eta}} \cdot S_{\hat{\eta} \hat{\eta}}^{-1} \cdot S_{\eta \hat{\eta}}^T = \Sigma_{\eta \eta} - \Sigma_{\eta \hat{\eta}} \cdot \Sigma_{\hat{\eta} \hat{\eta}}^{-1} \cdot \Sigma_{\eta \hat{\eta}}^T \quad (A17)$$

For sake of simplicity, these equalities will be demonstrated for one available forecast model. In this case only two variables are taken in account, η and $\hat{\eta}$, and their joint distribution is truncated over the variable $\hat{\eta}$ by the threshold value a . Hence, by substituting Eqs. (A10), (A11), (A13) and (A14), adapted for the specific case, in Eq. (A16) the following equation is obtained

$$\mu - \frac{\sigma_{\eta \hat{\eta}}}{\sqrt{\sigma_{\hat{\eta} \hat{\eta}}}} \cdot \lambda(\alpha) + \frac{\sigma_{\eta \hat{\eta}} + \frac{\sigma_{\eta \hat{\eta}} \cdot \sigma_{\hat{\eta} \hat{\eta}}}{\sigma_{\hat{\eta} \hat{\eta}}} \cdot \delta(\alpha)}{\sigma_{\hat{\eta} \hat{\eta}} + \frac{\sigma_{\hat{\eta} \hat{\eta}}^2}{\sigma_{\hat{\eta} \hat{\eta}}} \cdot \delta(\alpha)} \cdot \left[\hat{\eta}^* - \hat{\mu} + \frac{\sigma_{\hat{\eta} \hat{\eta}}}{\sqrt{\sigma_{\hat{\eta} \hat{\eta}}}} \cdot \lambda(\alpha) \right] = \mu + \frac{\sigma_{\eta \hat{\eta}}}{\sigma_{\hat{\eta} \hat{\eta}}} \cdot (\hat{\eta}^* - \hat{\mu}) \quad (A18)$$

Which can be rewritten as

$$\mu - \frac{\sigma_{\eta \hat{\eta}}}{\sqrt{\sigma_{\hat{\eta} \hat{\eta}}}} \cdot \lambda(\alpha) + \frac{\sigma_{\eta \hat{\eta}} \cdot \sigma_{\hat{\eta} \hat{\eta}} \cdot [1 + \delta(\alpha)]}{\sigma_{\hat{\eta} \hat{\eta}}^2 \cdot [1 + \delta(\alpha)]} \cdot [\hat{\eta}^* - \hat{\mu} + \sqrt{\sigma_{\hat{\eta} \hat{\eta}}} \cdot \lambda(\alpha)] = \mu + \frac{\sigma_{\eta \hat{\eta}}}{\sigma_{\hat{\eta} \hat{\eta}}} \cdot (\hat{\eta}^* - \hat{\mu}) \quad (A19)$$

Recent developments in predictive uncertainty assessment

G. Coccia and E. Todini

Title Page

Abstract

Introduction

Conclusions

References

Tables

Figures

◀

▶

◀

▶

Back

Close

Full Screen / Esc

Printer-friendly Version

Interactive Discussion



Recent developments in predictive uncertainty assessment

G. Coccia and E. Todini

Title Page

Abstract

Introduction

Conclusions

References

Tables

Figures

◀

▶

◀

▶

Back

Close

Full Screen / Esc

Printer-friendly Version

Interactive Discussion

By developing Eq. (A19) the following equality is obtained

$$\mu + \frac{\sigma_{\eta\hat{\eta}}}{\sigma_{\hat{\eta}\hat{\eta}}} \cdot (\hat{\eta}^* - \hat{\mu}) = \mu + \frac{\sigma_{\eta\hat{\eta}}}{\sigma_{\hat{\eta}\hat{\eta}}} \cdot (\hat{\eta}^* - \hat{\mu}) \quad (\text{A20})$$

Taking in account the Eq. (A17), it can be rewritten as

$$\sigma_{\eta\eta} + \frac{\sigma_{\eta\hat{\eta}}^2}{\sigma_{\hat{\eta}\hat{\eta}}} \cdot \delta(\alpha) - \frac{\left[\sigma_{\eta\hat{\eta}} + \frac{\sigma_{\eta\hat{\eta}} \cdot \sigma_{\hat{\eta}\hat{\eta}}}{\sigma_{\hat{\eta}\hat{\eta}}} \cdot \delta(\alpha) \right]^2}{\sigma_{\hat{\eta}\hat{\eta}} + \frac{\sigma_{\hat{\eta}\hat{\eta}}^2}{\sigma_{\hat{\eta}\hat{\eta}}} \cdot \delta(\alpha)} = \sigma_{\eta\eta} - \frac{\sigma_{\eta\hat{\eta}}^2}{\sigma_{\hat{\eta}\hat{\eta}}} \quad (\text{A21})$$

By developing it the following equation is obtained

$$\sigma_{\eta\eta} + \frac{\sigma_{\eta\hat{\eta}}^2}{\sigma_{\hat{\eta}\hat{\eta}}} \cdot \delta(\alpha) - \frac{\{\sigma_{\eta\hat{\eta}} \cdot \sigma_{\hat{\eta}\hat{\eta}} \cdot [1 + \delta(\alpha)]\}^2}{\sigma_{\hat{\eta}\hat{\eta}} \cdot \{\sigma_{\hat{\eta}\hat{\eta}}^2 \cdot [1 + \delta(\alpha)]\}} = \sigma_{\eta\eta} - \frac{\sigma_{\eta\hat{\eta}}^2}{\sigma_{\hat{\eta}\hat{\eta}}} \quad (\text{A22})$$

Which can be rewritten as

$$\sigma_{\eta\eta} + \frac{\sigma_{\eta\hat{\eta}}^2}{\sigma_{\hat{\eta}\hat{\eta}}} \cdot \delta(\alpha) - \frac{\sigma_{\eta\hat{\eta}}^2}{\sigma_{\hat{\eta}\hat{\eta}}} \cdot [1 + \delta(\alpha)] = \sigma_{\eta\eta} - \frac{\sigma_{\eta\hat{\eta}}^2}{\sigma_{\hat{\eta}\hat{\eta}}} \quad (\text{A23})$$

Now the equality is obtained

$$\sigma_{\eta\eta} - \frac{\sigma_{\eta\hat{\eta}}^2}{\sigma_{\hat{\eta}\hat{\eta}}} = \sigma_{\eta\eta} - \frac{\sigma_{\eta\hat{\eta}}^2}{\sigma_{\hat{\eta}\hat{\eta}}} \quad (\text{A24})$$

If considering the lower sample, only the second of the Eq. (A15) changes, while the other two expressions are still the same

$$\alpha_k = \frac{a_k - m_k}{\sqrt{S_{\hat{\eta}_k \hat{\eta}_k}}}$$

$$\lambda(\alpha) = -\frac{\phi(\alpha)}{\Phi(\alpha)} \quad (\text{A25})$$

$$\delta(\alpha) = \lambda(\alpha) \cdot [\lambda(\alpha) - \alpha]$$

The change in the form of $\lambda(\alpha)$ does not modify the previous procedure, which remains valid also for the lower sample and leads to the same result, with the only obvious difference that the sample moments are computed on the lower sample.

Acknowledgements. This work was supported by the Italian Ministry of Education. The authors thank C. Mazzetti and M. Martina for their guidance and advices. G. C. would like to thank C. Munera and F. Frances for providing the results and explanations of the TETIS model. GC also thanks L. Pujol for his support in developing the Artificial Neural Networks Model. Finally, the authors thank the NOAA's National Weather Service for providing all the data used in the case study.

References

- Coccia, G. and Todini E.: Application of a Bayesian processor for predictive uncertainty estimation in real time flood forecasting, BHS Third International Symposium, Role of hydrology in managing consequences of a changing global environment, Newcastle, 19 July, 2010. 9234
- De Groot, M. H.: Optimal Statistical Decision, McGraw-Hill, New York, 1970. 9221, 9222
- Dempster, A. P., Laird, N. M., and Rubin, D. B.: Maximum likelihood from incomplete data via the EM algorithm, J. R. Stat. Soc. B, 39, 1–39, 1977. 9227
- Edwards, A. L.: The correlation coefficient, in: An Introduction to Linear Regression and Correlation, chap. 4, W. H. Freeman, San Francisco, CA, 33–46, 1976.
- Frances, F., Velez, J. I., and Velez, J. J.: Split-parameter structure for the automatic calibration of distributed hydrological models, J. Hydrol., 332, 226–240, 2007 9242
- Kelly, K. S. and Krzysztofowicz, R.: A bivariate meta-Gaussian density for use in hydrology, Stoch. Hydrol. Hydraul., 11, 17–31, 1997.
- Koenker, R.: Quantile Regression, Econometric Society Monographs, Cambridge University Press, New York, NY, 2005. 9233
- Kohonen T.: The self-organizing map, Proceedings IEEE, 78(9), 1464–1480, doi:10.1109/5.58325, 1990. 9243
- Krzysztofowicz, R.: Bayesian theory of probabilistic forecasting via deterministic hydrologic model, Water Resour. Res., 35, 2739–2750, 1999. 9221, 9226, 9228
- Krzysztofowicz, R. and Kelly, K. S.: Hydrologic uncertainty processor for probabilistic river stage forecasting, Water Resour. Res., 36(11), 3265–3277, 2000. 9221

Recent developments in predictive uncertainty assessment

G. Coccia and E. Todini

Title Page

Abstract

Introduction

Conclusions

References

Tables

Figures



Back

Close

Full Screen / Esc

Printer-friendly Version

Interactive Discussion



Recent developments in predictive uncertainty assessment

G. Coccia and E. Todini

Title Page

Abstract

Introduction

Conclusions

References

Tables

Figures

⏪

⏩

◀

▶

Back

Close

Full Screen / Esc

Printer-friendly Version

Interactive Discussion



- Van der Waerden, B. L.: Order tests for two-sample problem and their power I, *Indagat. Math.*, 14, 453–458, 1952. 9228
- Van der Waerden, B. L.: Order tests for two-sample problem and their power II, *Indagat. Math.*, 15, 303–310, 1953a. 9228
- 5 Van der Waerden, B. L.: Order tests for two-sample problem and their power III, *Indagat. Math.*, 15, 311–316, 1953b. 9228
- Vélez, J. J., Puricelli, M., López Unzu, F., and Francés, F.: Parameter extrapolation to ungauged basins with a hydrological distributed model in a regional framework, *Hydrol. Earth Syst. Sci.*, 13, 229–246, doi:10.5194/hess-13-229-2009, 2009. 9242
- 10 Vrugt, J. A. and Robinson, B. A.: Treatment of uncertainty using ensemble methods: Comparison of sequential data assimilation and Bayesian model averaging, *Water Resour. Res.*, 43, W01411, doi:10.1029/2005WR004838, 2007. 9227
- Vrugt, J. A., Gupta, H. V., Bouten, W., and Sorooshian, S.: A Shuffled Complex Evolution Metropolis Algorithm for optimization and uncertainty assessment of hydrological model parameters, *Water Resour. Res.*, 39, 1201, doi:10.1029/2002WR001642, 2003. 9227
- 15 Weerts, A. H., Winsemius, H. C., and Verkade, J. S.: Estimation of predictive hydrological uncertainty using quantile regression: examples from the national flood forecasting system (England and Wales), *Hydrol. Earth Syst. Sci. Discuss.*, 7, 5547–5575, doi:10.5194/hessd-7-5547-2010, 2010. 9233
- 20 Werbos P.: Beyond Regression: New Tools for Prediction and Analysis in the Behavioral Science, Ph. D. dissertation, Harvard University, Cambridge, 1974. 9243
- Werbos P.: Generalization of backpropagation with application to a recurrent gas model, *Neural Networks*, 1, 339–356, 1988. 9243
- 25 Werbos P.: Backpropagation through time: What it does and how to do it, *Proc. IEEE*, 78(10), 1550–1560, 1990. 9243

Recent developments in predictive uncertainty assessment

G. Coccia and E. Todini

Table 1. Probability that the true value exceeds the $350 \text{ m}^3 \text{ s}^{-1}$ threshold when the expected value of prediction equals $250 \text{ m}^3 \text{ s}^{-1}$, computed for each model and their Bayesian combination.

$P(y > 350 \text{ m}^3 \text{ s}^{-1} \hat{y} = 250 \text{ m}^3 \text{ s}^{-1})$			
TOPKAPI	TETIS	ANN	3 MODELS
0.25	0.34	0.16	0.15

[Title Page](#)
[Abstract](#)
[Introduction](#)
[Conclusions](#)
[References](#)
[Tables](#)
[Figures](#)
[⏪](#)
[⏩](#)
[◀](#)
[▶](#)
[Back](#)
[Close](#)
[Full Screen / Esc](#)
[Printer-friendly Version](#)
[Interactive Discussion](#)

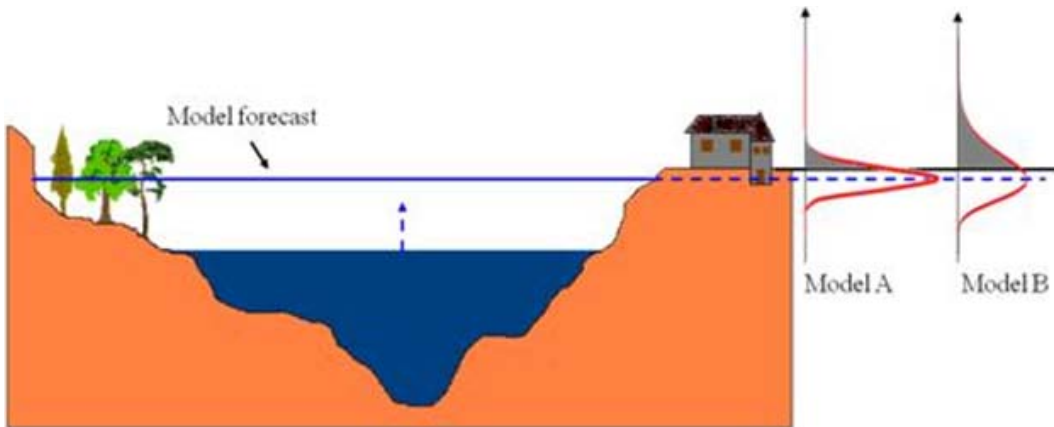



Fig. 1. Probability of exceeding the dyke level for the same expected value, forecasted by models with different reliability.

Recent developments in predictive uncertainty assessment

G. Coccia and E. Todini

Title Page

Abstract

Introduction

Conclusions

References

Tables

Figures

⏪

⏩

◀

▶

Back

Close

Full Screen / Esc

Printer-friendly Version

Interactive Discussion

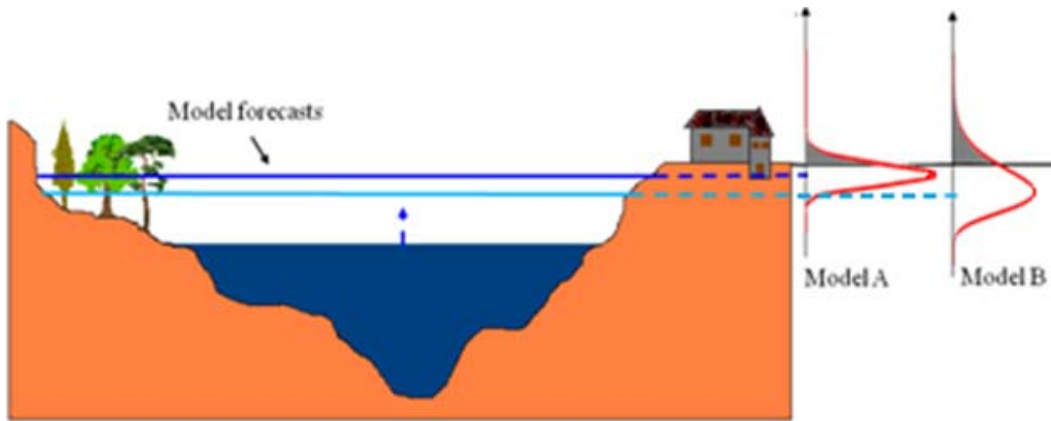


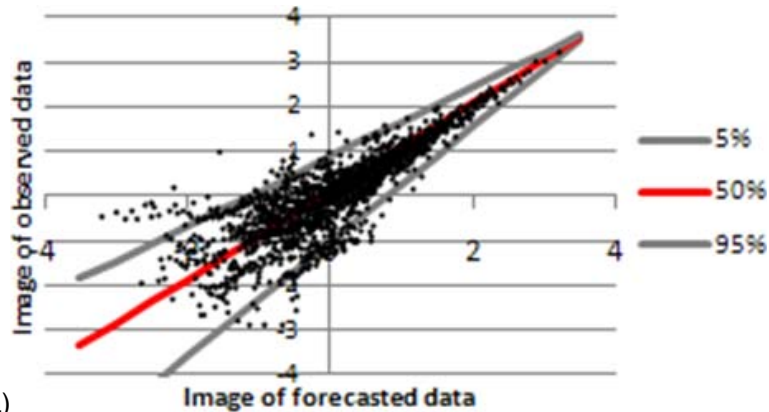
Fig. 2. Comparison between the expected value provided by models with different reliability when the probability of exceeding the dyke level is the same for all the models.

Recent developments in predictive uncertainty assessment

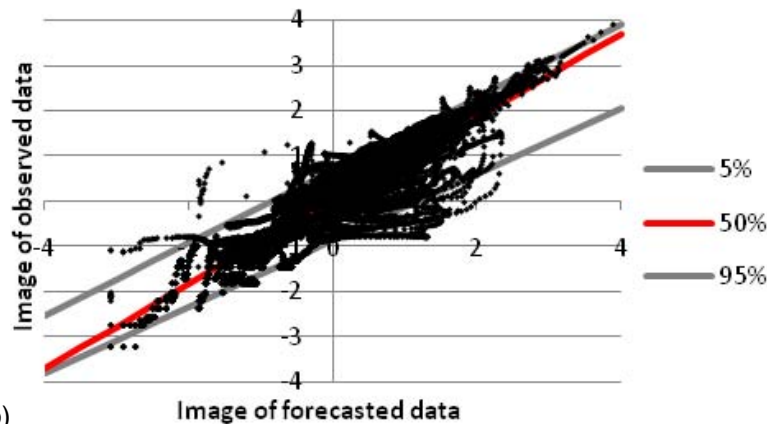
G. Coccia and E. Todini

Title Page	
Abstract	Introduction
Conclusions	References
Tables	Figures
◀	▶
◀	▶
Back	Close
Full Screen / Esc	
Printer-friendly Version	
Interactive Discussion	





(a)



(b)

Fig. 3. (a) An optimal situation for using the QR. (b) Poor results are obtained using QR in the situation represented here, which, by the way, is quite common in hydrological applications.

Recent developments in predictive uncertainty assessment

G. Coccia and E. Todini

Title Page

Abstract

Introduction

Conclusions

References

Tables

Figures

◀

▶

◀

▶

Back

Close

Full Screen / Esc

Printer-friendly Version

Interactive Discussion

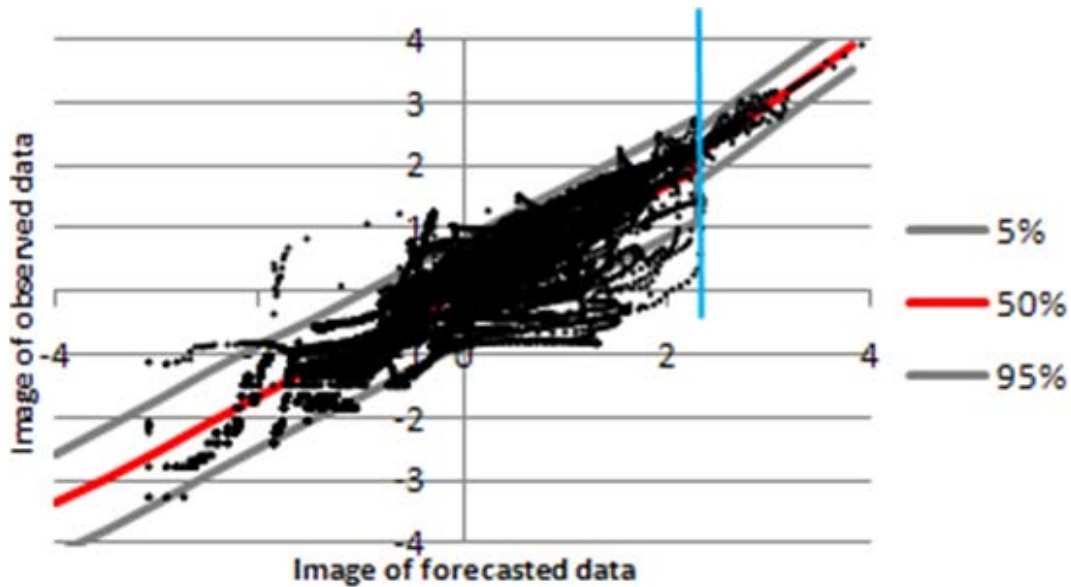


Fig. 4. Truncated normal joint distributions. The division of the Joint Distribution in the normal space into two bivariate truncated normal distributions is shown. The red line represents the modal value, while the grey lines represent the 5% and the 95% quantiles. The light blue line represents the threshold used in order to divide the two TNDs.

Recent developments in predictive uncertainty assessment

G. Coccia and E. Todini

Title Page

Abstract

Introduction

Conclusions

References

Tables

Figures

⏪

⏩

◀

▶

Back

Close

Full Screen / Esc

Printer-friendly Version

Interactive Discussion



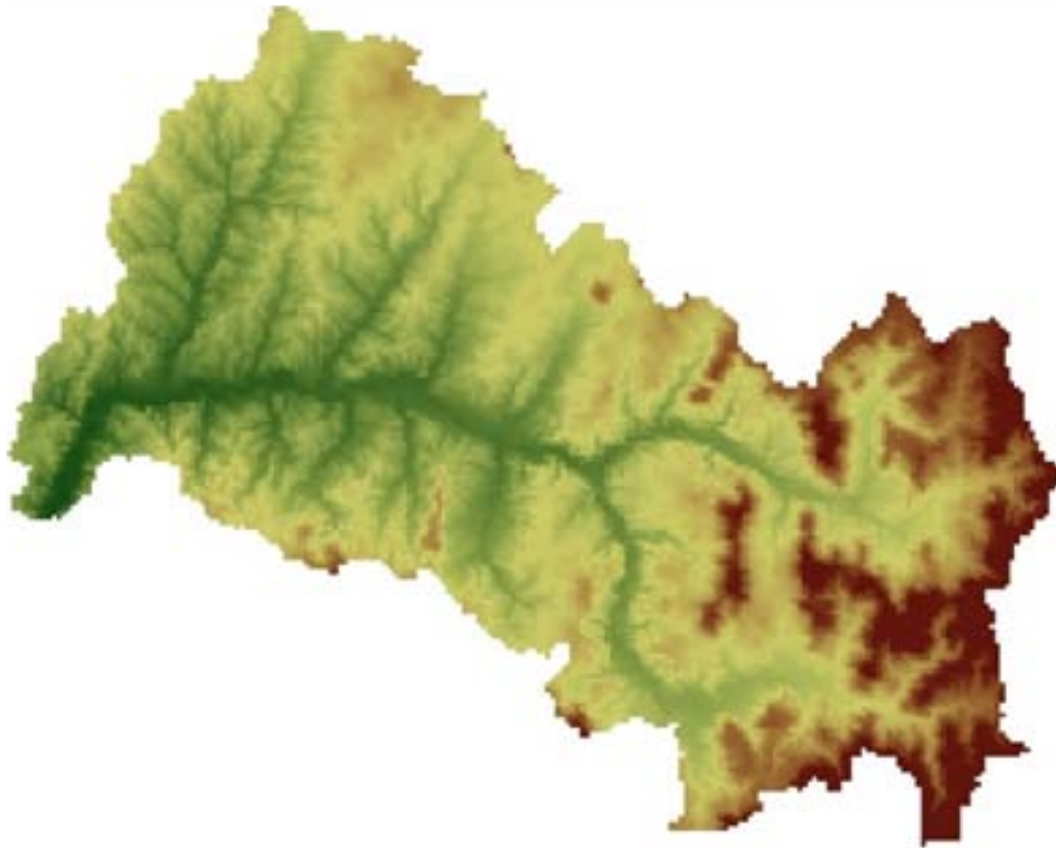


Fig. 5. Digital Elevation Model of the Baron Fork Basin closed at Eldon.

HESSD

7, 9219–9270, 2010

Recent developments in predictive uncertainty assessment

G. Coccia and E. Todini

Title Page

Abstract

Introduction

Conclusions

References

Tables

Figures



Back

Close

Full Screen / Esc

Printer-friendly Version

Interactive Discussion



Recent developments in predictive uncertainty assessment

G. Coccia and E. Todini

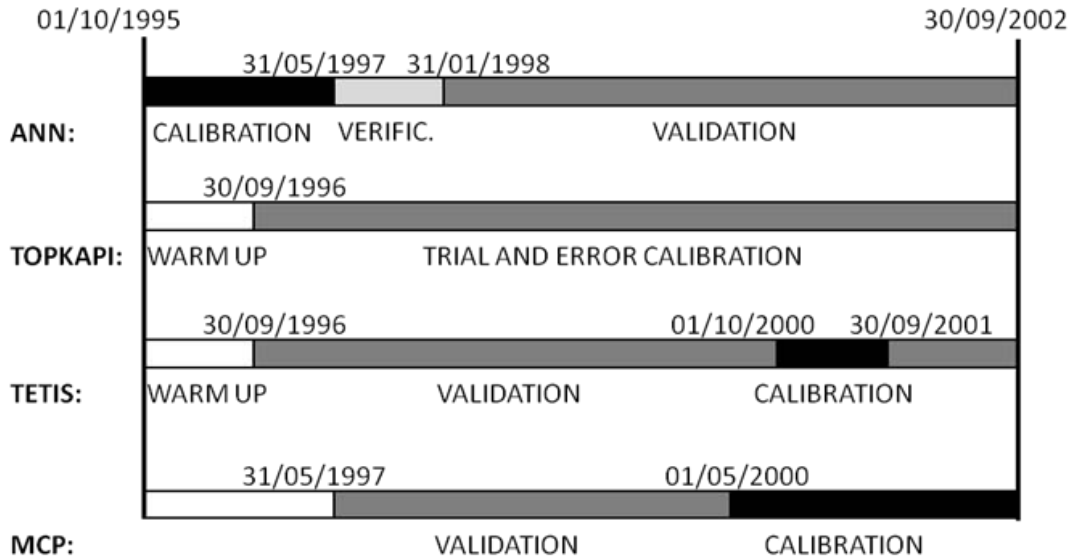


Fig. 6. Schematization of the available data division for calibrating and validating the models and the MCP.

Title Page

Abstract

Introduction

Conclusions

References

Tables

Figures

⏪

⏩

◀

▶

Back

Close

Full Screen / Esc

Printer-friendly Version

Interactive Discussion



Recent developments in predictive uncertainty assessment

G. Coccia and E. Todini

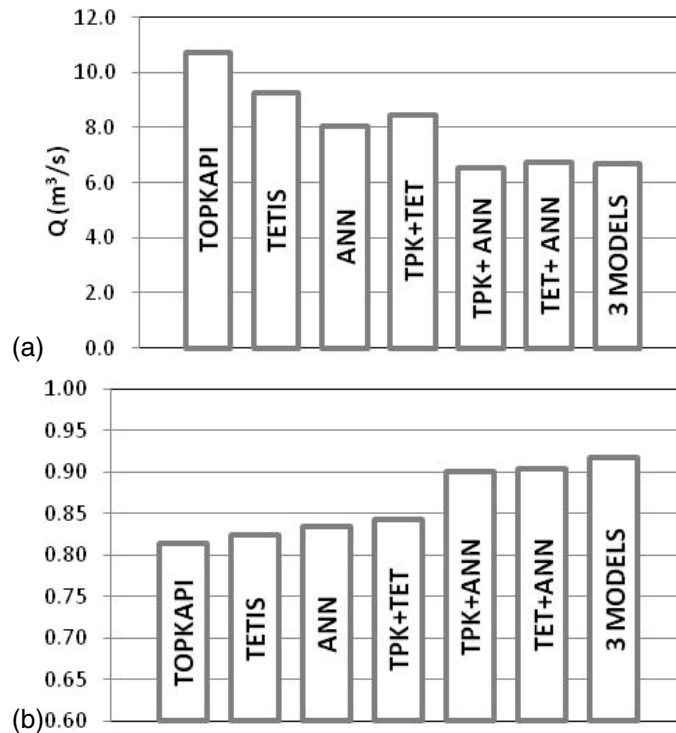


Fig. 7. (a) Error Standard Deviation for Topkapi model (TPK), Tetis model (TET), ANN model and their combinations during the entire validation period of the MCP. (b) Nash-Sutcliffe coefficient for Topkapi model (TPK), Tetis model (TET), ANN model and their combinations during the entire validation period of the MCP.

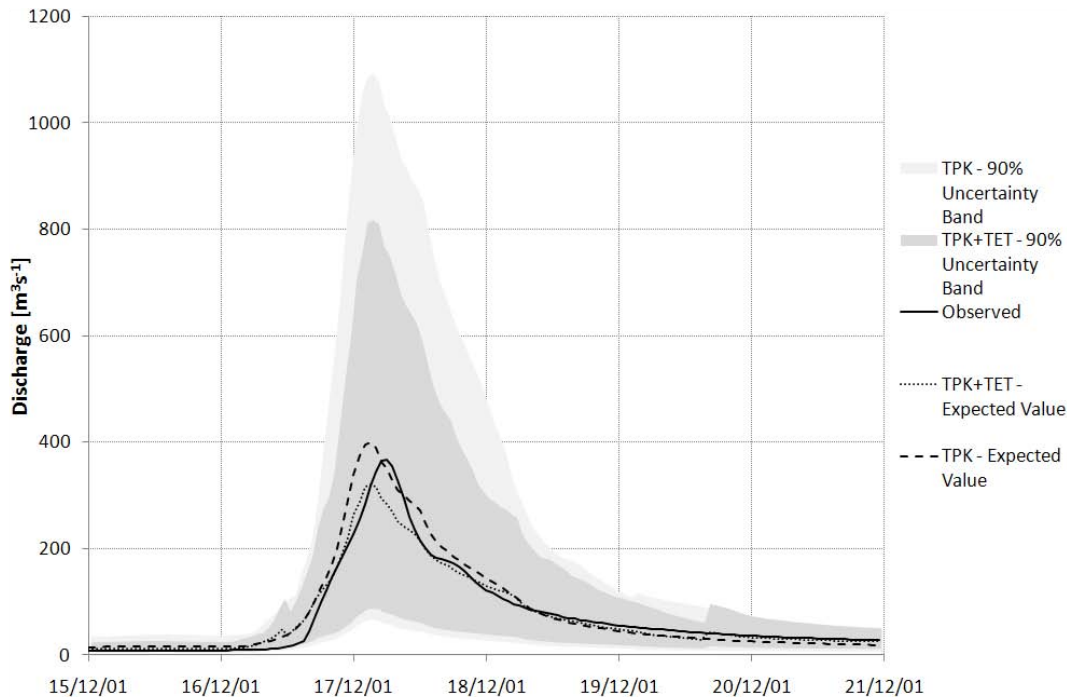


Fig. 8. Comparison between the PU computed with one or two models on a flood event during calibration period. Observed discharges (black line); expected value conditioned only to the Topkapi forecast (dashed line); expected value conditioned to the Topkapi and Tetis forecasts (dotted line); 90% uncertainty band conditioned to the Topkapi forecast (light grey band); 90% uncertainty band conditioned to the Topkapi and Tetis forecasts (grey band).

Recent developments in predictive uncertainty assessment

G. Coccia and E. Todini

- Title Page
- Abstract
- Introduction
- Conclusions
- References
- Tables
- Figures
- ⏪
- ⏩
- ◀
- ▶
- Back
- Close
- Full Screen / Esc
- Printer-friendly Version
- Interactive Discussion

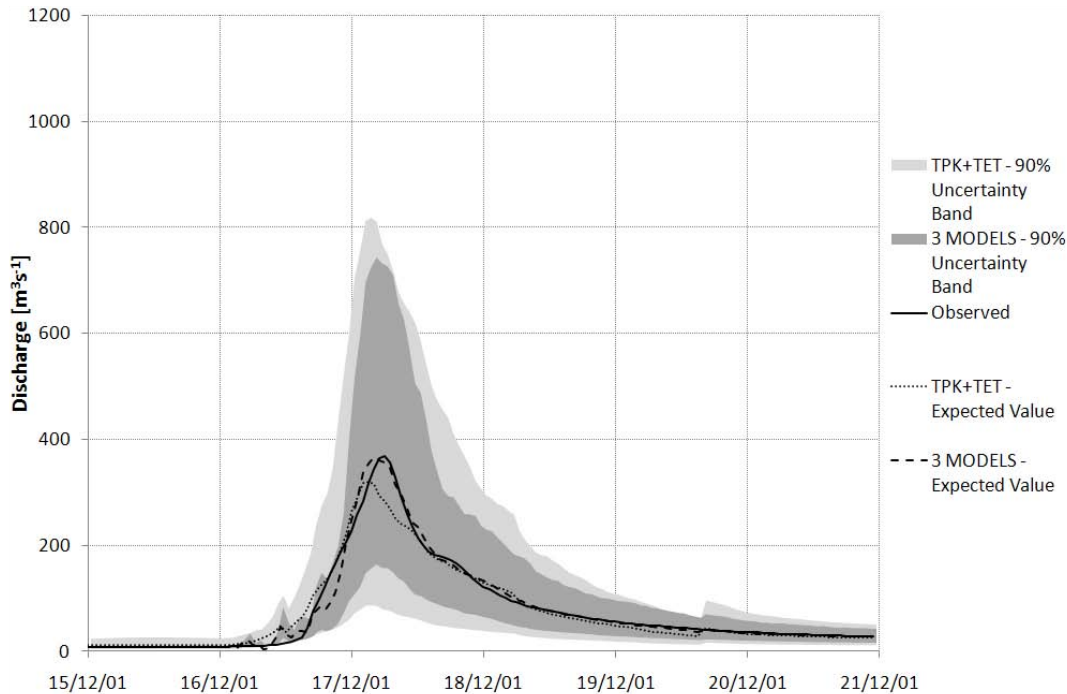


Fig. 9. Comparison between the PU computed combining, two or three models on a flood event during calibration period. Observed discharges (black line); expected value conditioned only to the Topkapi and Tetis forecasts (dotted line); expected value conditioned to the Topkapi, Tetis and Ann forecasts (dashed line); 90% uncertainty band conditioned to the Topkapi and Tetis forecasts (light grey band); 90% uncertainty band conditioned to the Topkapi, Tetis and Ann forecasts (grey band).

Recent developments in predictive uncertainty assessment

G. Coccia and E. Todini

[Title Page](#)

[Abstract](#) [Introduction](#)

[Conclusions](#) [References](#)

[Tables](#) [Figures](#)

[⏪](#) [⏩](#)

[◀](#) [▶](#)

[Back](#) [Close](#)

[Full Screen / Esc](#)

[Printer-friendly Version](#)

[Interactive Discussion](#)



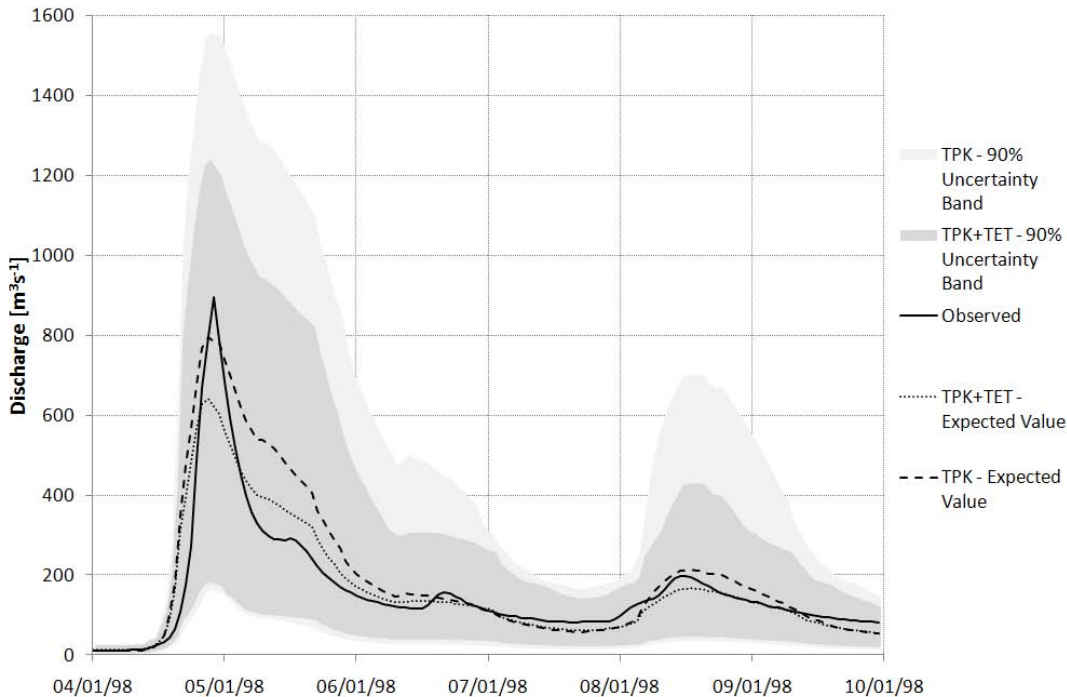


Fig. 10. Comparison between the PU computed with one or two models on a flood event during validation period. Observed discharges (black line); expected value conditioned only to the Topkapi forecast (dashed line); expected value conditioned to the Topkapi and Tetis forecasts (dotted line); 90% uncertainty band conditioned to the Topkapi forecast (light grey band); 90% uncertainty band conditioned to the Topkapi and Tetis forecasts (grey band).

Recent developments in predictive uncertainty assessment

G. Coccia and E. Todini

[Title Page](#)

Abstract	Introduction
Conclusions	References
Tables	Figures

⏪
⏩

◀
▶

Back	Close
----------------------	-----------------------

[Full Screen / Esc](#)

[Printer-friendly Version](#)

[Interactive Discussion](#)



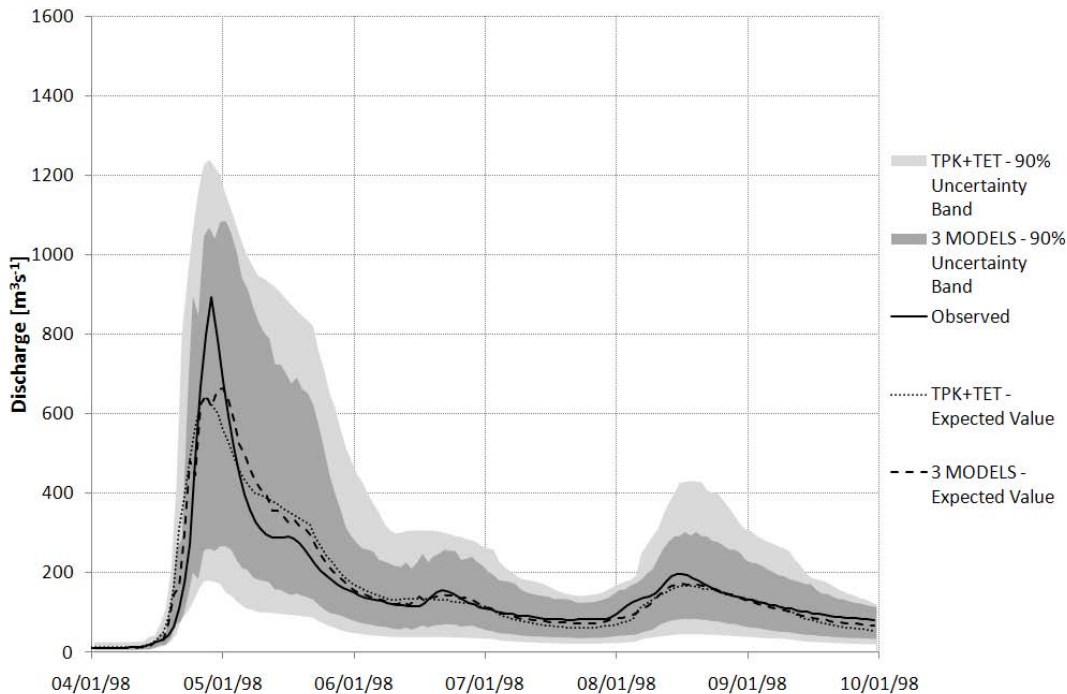


Fig. 11. Comparison between the PU computed combining, two or three models on a flood event during validation period. Observed discharges (black line); expected value conditioned only to the Topkapi and Tetis forecasts (dotted line); expected value conditioned to the Topkapi, Tetis and Ann forecasts (dashed line); 90% uncertainty band conditioned to the Topkapi and Tetis forecasts (light grey band); 90% uncertainty band conditioned to the Topkapi, Tetis and Ann forecasts (grey band).

**Recent developments
in predictive
uncertainty
assessment**

G. Coccia and E. Todini

[Title Page](#)

[Abstract](#) [Introduction](#)

[Conclusions](#) [References](#)

[Tables](#) [Figures](#)

[⏪](#) [⏩](#)

[◀](#) [▶](#)

[Back](#) [Close](#)

[Full Screen / Esc](#)

[Printer-friendly Version](#)

[Interactive Discussion](#)



Recent developments in predictive uncertainty assessment

G. Coccia and E. Todini

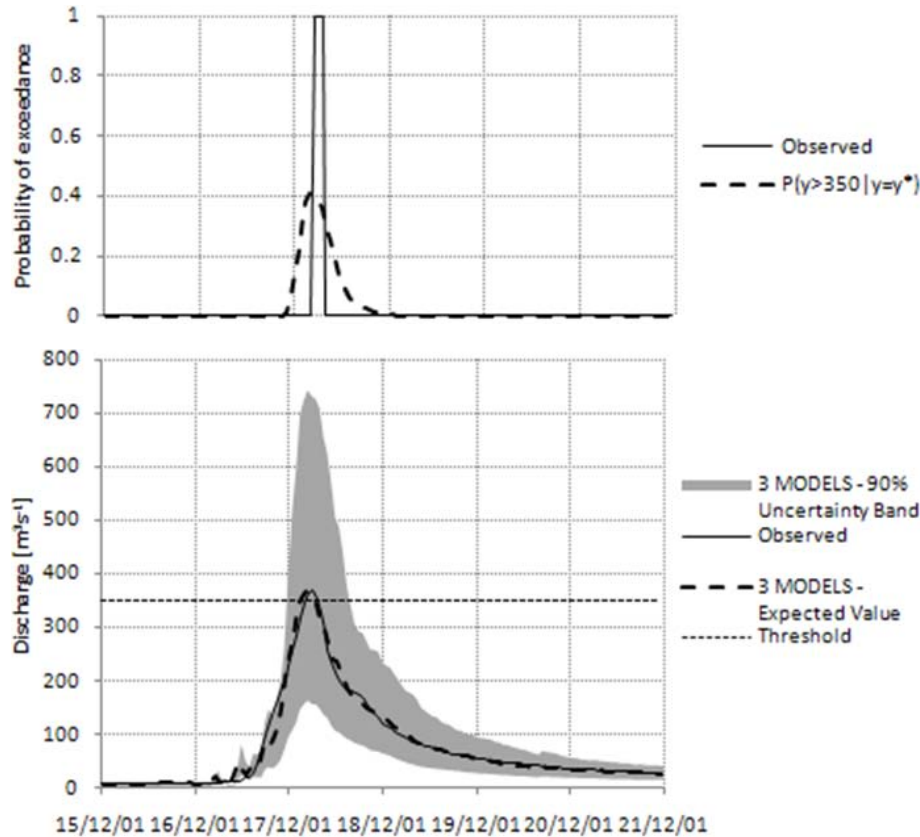


Fig. 12. Flood event during calibration period. The lower part represents the discharge forecast; observed values (continuous line); expected value conditioned to the Topkapi, Tetis and Ann forecasts (dashed line); 90% uncertainty band (grey area); alarm threshold of $350 \text{ m}^3 \text{ s}^{-1}$ (small dashed line). The upper part represents the probability of exceeding the alarm threshold; observed binary response (continuous line) and Probability of exceeding the threshold computed by the MCP (dashed line).

[Title Page](#)
[Abstract](#)
[Introduction](#)
[Conclusions](#)
[References](#)
[Tables](#)
[Figures](#)
[◀](#)
[▶](#)
[◀](#)
[▶](#)
[Back](#)
[Close](#)
[Full Screen / Esc](#)
[Printer-friendly Version](#)
[Interactive Discussion](#)

Recent developments in predictive uncertainty assessment

G. Coccia and E. Todini

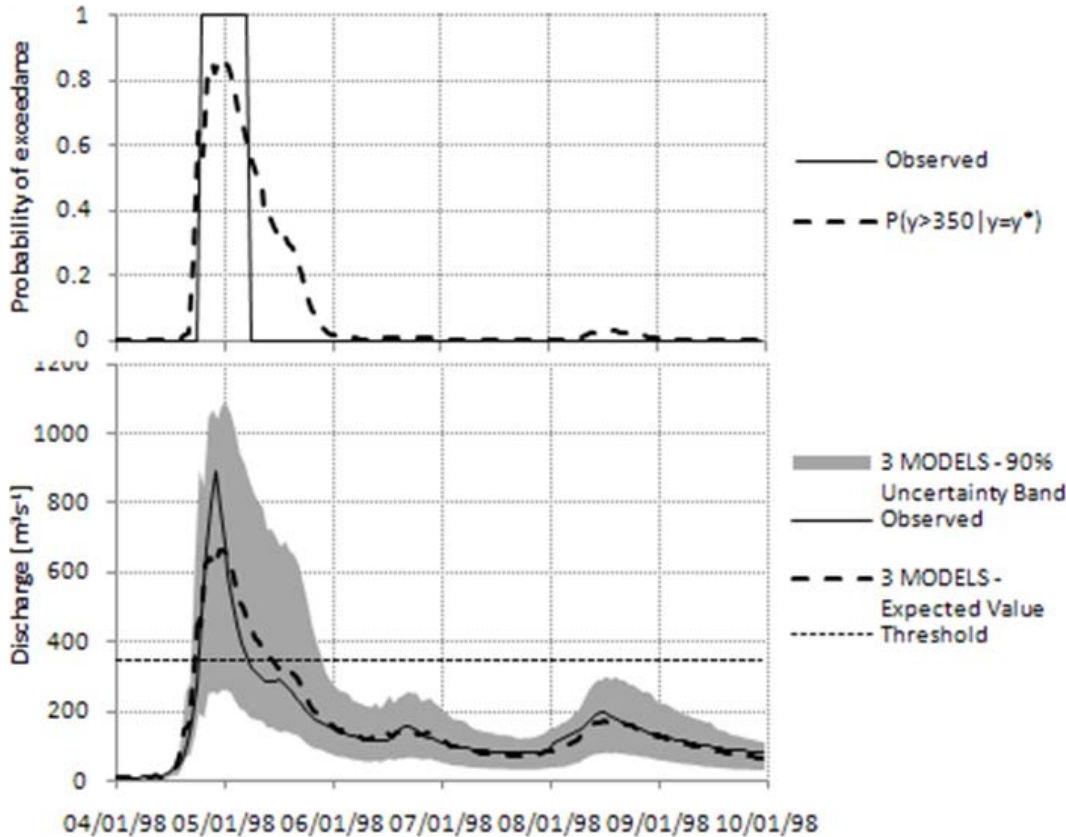


Fig. 13. Flood event during validation period. The lower part represents the discharge forecast; observed values (continuous line); expected value conditioned to the Topkapi, Tetis and Ann forecasts (dashed line); 90% uncertainty band (grey area); alarm threshold of $350 \text{ m}^3 \text{ s}^{-1}$ (small dashed line). The upper part represents the probability of exceeding the alarm threshold; observed binary response (continuous line) and Probability of exceeding the threshold computed by the MCP (dashed line).

Title Page

Abstract	Introduction
Conclusions	References
Tables	Figures

⏪ ⏩
◀ ▶
Back Close

Full Screen / Esc

Printer-friendly Version

Interactive Discussion



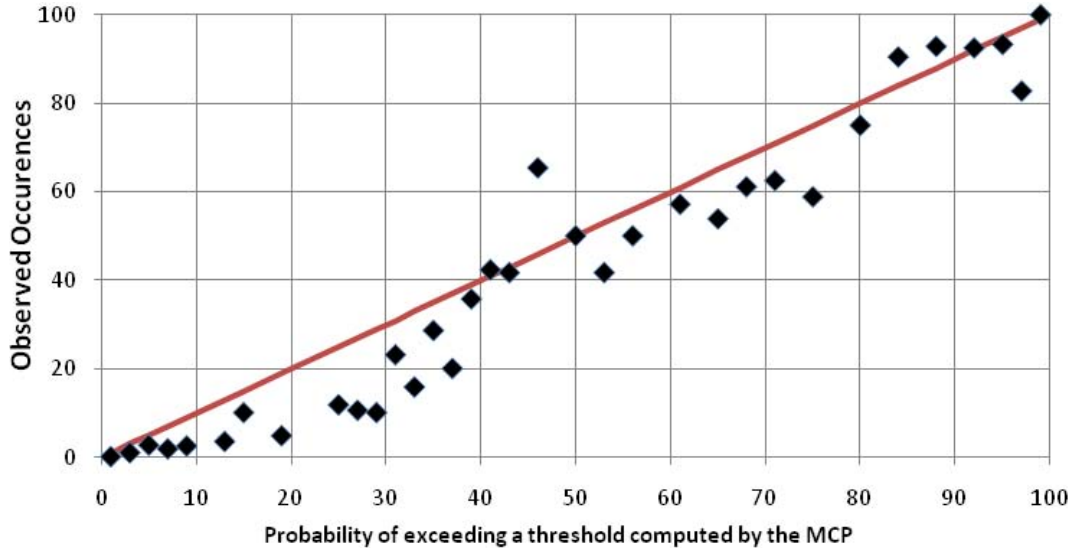


Fig. 14. Frequency of actual threshold exceedances vs. the probability estimated using the MCP Bayesian combination of the three models. The red line represents the perfect behaviour.

Recent developments in predictive uncertainty assessment

G. Coccia and E. Todini

Title Page

Abstract	Introduction
Conclusions	References
Tables	Figures

⏪	⏩
◀	▶
Back	Close

Full Screen / Esc

Printer-friendly Version

Interactive Discussion

